intensity vs time after probe injection. Tiron or dimethylthiourea (DMTU) (3 μmol/mouse, dissolved in saline) was administered simultaneously with the probe to confirm the relationship between the signal decay and ROS generation.

Statistical analysis

All data are expressed as mean ± SEM. Between-group comparisons of the means were performed by one-way ANOVA followed by *t*-tests. Bonferroni's correction was done for multiple comparisons of means. A *p*-value less than 0.05 was considered to be statistically significant.

Results

Animal characteristics

The echocardiographic data of surviving mice at days 1, 4, 7, 14 and 28 after MI and control mice are shown in Table I. LV diameters were significantly greater in MI mice at day 4 and thereafter compared to sham-operated control mice. Moreover, MI mice had smaller fractional shortening and anterior wall thickness. There were no alterations in LV diameter and systolic function in sham-operated mice without coronary artery ligation up to day 28 after the operation (data not shown). At day 28, left ventricule LV end-diastolic pressure (LVEDP) was increased in MI (2.6 ± 0.7 vs 14.0 ± 2.3, $p < 0.01$) and LV weight (wt)/body wt (3.12 ± 0.11 vs 3.68 ± 0.17 mg/g, $p < 0.05$), RV wt/body wt (0.88 ± 0.06 vs 1.38 ± 0.11 mg/g, $p < 0.05$), lung wt/body wt (5.36 ± 0.13 vs 7.71 ± 0.80 mg/g, $p < 0.05$) were all increased in MI. The prevalence of pleural effusion was significantly higher in MI (0 vs 50%, $p < 0.01$).

Oxidative byproducts in plasma and urine

Plasma TBARS and urinary 8-OH-dG were significantly elevated at day 1 after MI (Figure 1), and declined to control levels at day 7 and thereafter.

Oxidative markers and antioxidant enzyme activity in myocardial tissue

We measured TBARS (an indicator of lipid peroxidation) and performed immunohistochemical staining of HEL in both infarct and non-infarct myocardial samples. In the infarct area, TBARS increased at day 1 and 7 after MI (Figure 2A). In the non-infarct area, on the contrary, TBARS level was not altered in the early days (days 1, 7 and 14) after MI but was elevated only at day 28.

In agreement with the results of myocardial TBARS, HEL-positive cardiomyocytes were located in the infarct area, whereas there was no staining in the non-infarct area at day 4. (Figure 3). HEL is a novel lipid hydroperoxide modified lysine residue, which is formed by oxidative modification by oxidized ω6 fatty acids such as linoleic acid or arachidonic acid. HEL is a useful biomarker for the initial stage of lipid peroxidation. Although positive staining lasted in the infarct area at day 28, the myocardium was mostly replaced by fibrous tissue and little living myocyte existed. In the non-infarct area, cardiomyocytes were hypertrophied and positively stained by HEL antibody. These suggest that lipid peroxidation starts at an early stage in the infarct area but at late remodelling stage in the non-infarct area. This is consistent with TBARS level in myocardium and indicated increased generation of ROS in the non-infarct area at day 28. The increase of TBARS in the non-infarct area was associated with a significant decline in SOD activity and a tendency of decrease in GPx activity at day 28 (Figure 4).

In vivo *ESR in the heart*

Since TBARS is known to be a non-specific assay to measure lipid peroxidation from biological fluids and tissues and many other substances besides reactive aldehydes react with TBA, we used *in vivo* ESR to determine whether the level of ROS increased in the heart in the remodelling process. Methoxycarbonyl-PROXYL, a stable membrane-permeable nitroxyl radical, is converted into its non-magnetic products, such as its hydroxylamine, immediately after the

Table I. Echocardiographic data.

		Time after MI (days)				
	Control	1	4	7	14	28
n	7	6	6	10	9	8
Heart rate (bpm)	524 ± 22	564 ± 25	552 ± 16	568 ± 23	551 ± 28	589 ± 43
LVEDD (mm)	4.0 ± 0.2	4.5 ± 0.2	5.0 ± 0.2**	5.1 ± 0.2**	5.4 ± 0.1**	5.6 ± 0.2**
LVESD (mm)	2.3 ± 0.2	3.6 ± 0.2**	3.9 ± 0.2**	3.9 ± 0.1**	4.2 ± 0.1**	4.4 ± 0.1**
Fractional shortening (%)	37.6 ± 1.6	21.1 ± 1.6**	22.2 ± 1.6**	23.2 ± 1.6**	20.7 ± 1.0**	21.0 ± 2.7**
Infarct wall thickness (mm)	0.83 ± 0.03	0.60 ± 0.05**	0.61 ± 0.03**	0.44 ± 0.02**	0.44 ± 0.06**	0.30 ± 0.08**
Non-infarct wall thickness (mm)	0.84 ± 0.04	0.80 ± 0.05	1.00 ± 0.02	1.13 ± 0.07*	1.30 ± 0.05**	1.25 ± 0.18**

Control, sham-operated mice; LV, left ventiruclar; EDD, end-diastolic dimension; ESD, end-systolic dimension.
Values are means ± SEM. * $p < 0.05$, ** $p < 0.01$ vs controls.

Downloaded By: [Kyushu University Central Library] At: 03:45 11 May 2009

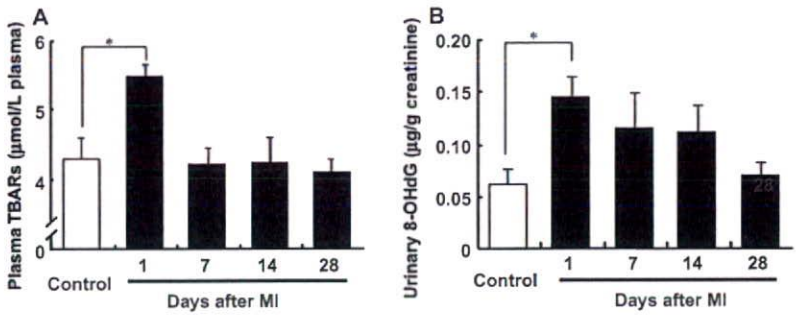

Figure 1. Time-dependent changes of plasma TBARs (A) and urinary 8-OHdG (B) in sham-operated control mice ($n=7$) and mice on day 1 ($n=6$), day 7 ($n=10$), day 14 ($n=9$) and day 28 ($n=8$) after MI. Values are means ± SEM. * $p<0.05$, ** $p<0.01$ compared with sham-operated control.

reaction with hydroxy radicals or other reductants. To determine the level of ROS or redox status by *in vivo* ESR measurements, we used methoxycarbonyl-PROXYL as a spin probe which was observed as three sharp lines by ESR spectroscopy (Figure 5A).

We applied signal decay of methoxycarbonyl-PROXYL to *in vivo* ESR to measure ROS generation non-invasively in the failing heart in mice after MI. When the ESR spectrum was measured at the chest level, the signal decay rate was greater in MI mice than sham-operated mice (Figure 5B). The increase of the signal decay observed in MI was suppressed by a simultaneous injection of antioxidants, Tiron or DMTU (Figure 5C and D), indicating the enhancement of free radical reactions at the chest in MI mice. To confirm that the enhancement of signal decay is localized at the chest and does not reflect the increase of systemic free radical generation, the same ESR measurement was repeated at the other parts of the body, head and abdomen from the same animals. ESR signal decay was similar between the two groups when the spectrum was detected at the head and abdominal levels (Figure 5E and F).

Redox alteration during the process of remodelling after MI

Using this *in vivo* ESR technique, we measured free radical production during the time course of remodelling after MI in mice. Radical generation was increased gradually in 4 weeks after MI, which was in parallel to the increase of LVEDD and LVESD and the decrease of EF assessed by echocardiography (Figure 6).

Discussion

In the post-MI myocardium, early remodelling occurs accompanied by infarct expansion, regional dilatation and thinning of the infarct zone and is followed by further deterioration in cardiac performance and increased neurohormonal activation in late remodelling. ROS play an important role in the progression of remodelling in the post-MI myocardium. However, phase-dependent alteration of ROS production in the post-MI myocardium has not been discussed. Moreover, despite a lack of evidence, it is widely misconstrued that an increase of local ROS production is reflected by increases of systemic ROS markers. The present study demonstrates that systemic elevations of ROS markers occur only at the earlier phase after MI. On the contrary, the generation of ROS in non-infarct myocardium is increased from the late phase.

Roles of ROS in the progression of cardiac remodelling

ROS potentially cause cellular damage and dysfunction. Whether the effects of ROS are beneficial or

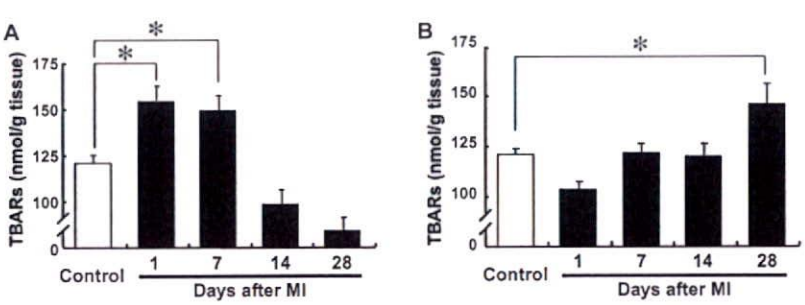

Figure 2. Time-dependent changes of TBARs in infarct (A) and in non-infarct (B) myocardium in sham-operated control ($n=7$) and on day 1 ($n=6$), day 7 ($n=10$), day 14 ($n=9$) and day 28 ($n=8$) after MI. Values are means ± SEM. * $p<0.05$ compared with sham-operated control.

Downloaded By: [Kyushu University Central Library] At: 03:45 11 May 2009

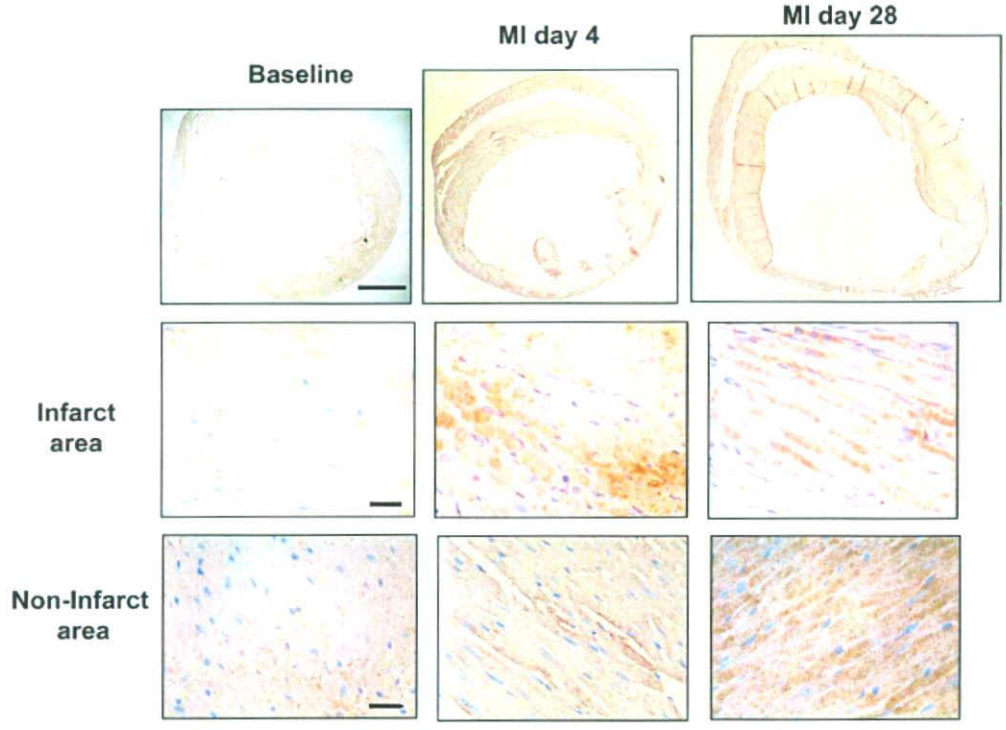

Figure 3. Immunohistochemical detection of HEL moieties in the remodelling process in whole LV, infarct myocardium and non-infarct myocardium, during acute-phase (day 4) and late-phase (day 28) after MI. Scale bar; 1 mm (top) and 10 μm (infarct area and non-infarct area).

harmful depends on the site of action, the source, the amount of ROS generation and the resulting redox balance. Several groups reported that ROS are increased in congestive HF patients [27,28] and accumulating evidence from animal studies revealed that increased ROS play a pivotal role in the pathogenesis and progression of HF [4,9,29–33]. However, whether systemic ROS markers are useful for determining the redox state of the failing heart remains unknown. Li et al. [34] used LC/MS/MS to analyse F_2-isoprostanes in urine from HF patients. They found that only a few peaks were increased, but the most abundant isomer 5-epi-8,12-iso-iPF$_{2\alpha}$-VI was comparable to control subjects. Other clinical studies examined ROS in serum or urine in HF patients by measuring redox markers and reported that ROS are elevated in functionally very poor, NYHA class III or class IV patients. At the time of acute deterioration of HF or sudden onset of cardiac ischemia, patients often have congestion or elevation of LV end diastolic pressure. In such conditions, the immune system, neurohormonal factors such as TNFα and other cytokines are activated with concurrent activation of sympathetic nerve, all of which cause endothelial damage and other organ disorders [35]. In fact, acute MI is associated with a marked increase of inflammatory cells. Previous reports have demonstrated that inflammatory responses and neurohormonal factors cause the generation of oxidative stress not only from the myocardium but also from the vasculature [36–40]. These observations are consistent with our result showing that alteration of systemic ROS markers may not always reflect ROS generation in the myocardium.

Redox status estimated by in vivo ESR

ESR spectroscopy is a useful method to estimate redox status in living animals. In this study, we demonstrated using *in vivo* ESR spectroscopy that increased generation of free radicals in the heart correlated with dilatation of LV and decrease in EF, both of which are indices of the myocardial remodelling process after MI.

There are several advantages to determine ROS generation by *in vivo* ESR spectroscopy. First, the method allows non-invasive assessment of ROS generation in an *in vivo* setting. Secondly, *in vivo* ESR can be repeated in the same animal at different time points, indicating that the ESR technique has the potential to be used as a diagnostic tool in the future. Thirdly, this ESR technique can estimate and quantify the 'net' redox state. Antioxidant enzymes and reductants (such as glutathione) in the ROS generating system together determine the total redox status in biological systems, which may change dynamically and acutely in the heart after MI. Byproducts of free oxygen radicals such as lipid

Downloaded By: [Kyushu University Central Library] At: 03:45 11 May 2009

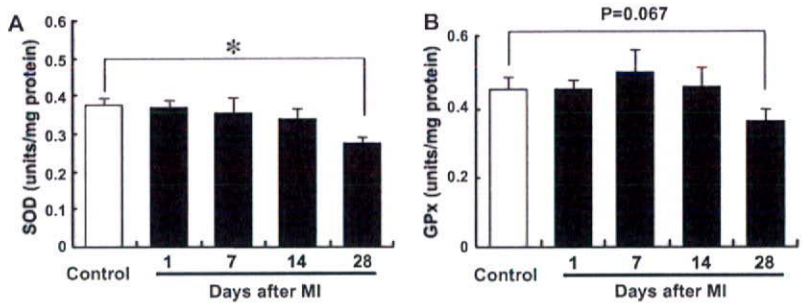

Figure 4. Time-dependent changes of activities of SOD (A) and GPx (B) in non-infarcted myocardium from sham-operated control ($n=7$) and on day 1 ($n=6$), day 7 ($n=10$), day 14 ($n=9$) and day 28 ($n=8$) after MI. Values are means ± SEM. * $p<0.05$ compared with sham-operated control.

Downloaded By: [Kyushu University Central Library] At: 03:45 11 May 2009

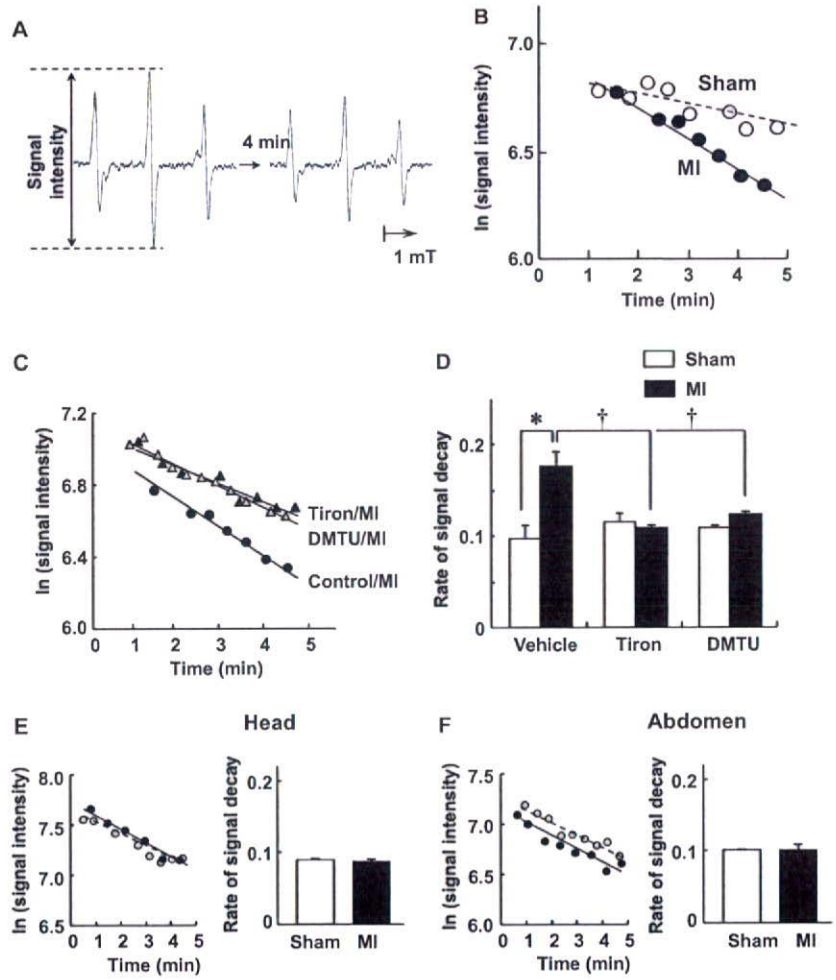

Figure 5. (A) A representative ESR signal of methoxycarbonyl-PROXYL at the chest level of a mouse with myocardial infarction (MI). (B) Semilogarithmic plots of the peak heights of the ESR spectra of methoxycarbonyl-PROXYL after spin probe injection. The signal intensity declined with time, which is defined as the signal decay. (C) The effects of addition of free radical scavengers on the rate of signal decay measured by *in vivo* ESR spectroscopy in individual MI mice. Tiron (a superoxide scavenger) or dimetylthiourea (DMTU; a hydroxyradical scavenger) was injected simultaneously with the injection of methoxycarbonyl-PROXYL. (D) Rates of signal decay measured by *in vivo* ESR in sham and MI groups in the absence and presence of radical scavengers ($n=6$ in each group). *$p<0.01$ vs sham-vehicle group and †$p<0.01$ vs MI-vehicle group. Values are means ± SEM. (E, F) Representative plots of individual mice and rates of *in vivo* ESR signal decay in sham and MI groups ($n=5$ each) measured at the head (E) and abdomen (F).

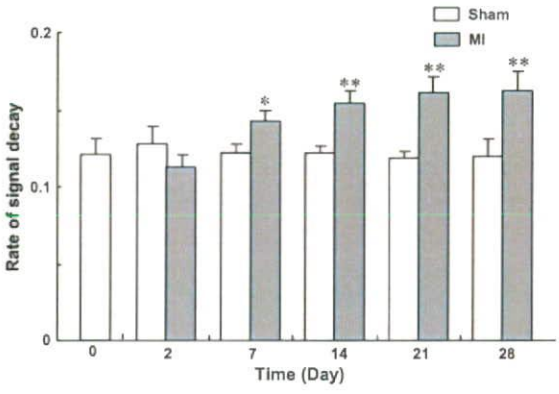

Figure 6. Changes in the rates of signal decay over time measured by *in vivo* ESR spectroscopy in sham and MI mice at days 0, 2, 7, 14 and 28 after operation ($n = 7$ in each group). Values are means ±SEM. $*p < 0.05$, $**p < .01$ vs sham values for the rate of signal decay.

peroxide, products of protein modifications and DNA damage do not always represent the net capacity of ROS reactions and do not necessary reflect ROS generation in specific organs or tissue. Difficulty in the interpretation of enhanced signal decay has been pointed out, because the nitroxyl radicals are known to react with not only free radicals but also other reductants including ascorbic acid and glutathione. However, we found that the increased ESR signal decay in heart failure was normalized by the addition of Tiron and DMTU. Furthermore, the TBARs study provided evidence that the ESR data reflect the increase of ROS in the failing heart, all of which support that the enhancement of signal decay in late remodelling represents at least the alteration of total redox status in the myocardium, most probably due to an increase of ROS.

Alteration of antioxidants and lipid peroxidation in non-infarct myocardium

We found that ROS markers including both byproducts of ROS and antioxidant enzymes were altered concomitantly in urine and blood at the early phase after MI and were normalized at the late remodelling state at 28 days post-MI. An increase of lipid peroxidation indicated by TBARS in infarct myocardium coincided with these systemic alterations (Figures 1 and 2). On the contrary, with the progression of remodelling represented by LV dilatation and reduced ejection fraction, the TBARS level in non-infarct myocardium increased at day 28. The immunohistochemical analysis by HEL antigen substantiated the finding that ROS was increased in the non-infarct myocardium during late remodelling. It is consistent with our previous findings in a tachycardia-induced canine HF model, in which ROS generation was enhanced in the failing myocardium and correlated with LV end-diastolic pressure and LV ejection fraction [41]. Nevertheless, it remains unknown why oxidative stress was not detectable in urine or in blood in late remodelling after MI, even with the progression of remodelling. A possible explanation is the differences in the source and amount of ROS between the early phase and the chronic phase of HF. In the later phase of post-MI remodelling, ROS increase may occur mainly in the myocardium and multiple defense mechanisms against ROS stabilize the levels in blood and urine. Moreover, ROS is so short-lived that it may not be possible to detect them in urine or blood when the source is localized in a single organ. In contrast, systemic inflammatory responses manifested clinically as leukocytosis and increased cytokines during acute deterioration or sudden ischemia [42–46] may not have enough time to cope with the acute ROS attack and redox change. We suspect that the acute increase in systemic ROS markers after MI is due to systemic activation of inflammatory cells. However, while administration of cyclophosphamide depletes leukocytes by 93% [15,47], the drug inhibited TBARS only partially by ~ 48% (data not shown). This indicates that sources other than leukocytes, such as vasculature, may contribute to systemic ROS generation in the acute phase of MI. All of these results suggest the difficulties of detecting ROS in blood or urine by specific markers in chronic HF, even with enhanced production of ROS from the remodelling myocardium.

Among the many detection techniques of ROS markers available currently, the most sensitive method is the detection of isoprostanes by mass spectroscopy. However, it is known that most of the major peaks of isoprostanes are not elevated in urine from HF patients [30]. Furthermore, commercially available ELISA kits are not as reliable as GC-MS assay [48]. Therefore, we measured a sensitive but not very specific marker TBARS for estimating ROS in plasma.

Clinical implications

Our study suggests that the increased local production of ROS is not always reflected in blood or urine during progression of remodelling. ROS are extremely unstable and difficult to detect directly. The establishment of a non-invasive method to detect ROS generated locally in the remodelling myocardium may permit time- and tissue-targeted therapy for more effective treatment of remodelling and failing heart.

Conclusion

We demonstrated that the generation of ROS in the non-infarct myocardium increases with the progression of cardiac remodelling and this increase is not

Downloaded By: [Kyushu University Central Library] At: 01:45 11 May 2009

reflected by the levels of ROS markers in blood and urine. Clarification of the mechanisms of ROS-mediated remodelling and targeting non-infarct myocardium may lead to novel and effective therapeutic strategies for HF.

Acknowledgements

This study was supported in part by the Uehara memorial foundation and grants from the Ministry of Education (181-00006). A part of this study was conducted in Kyushu University Station for Collaborative Research II.

***Declaration of interest*:** The authors report no conflicts of interest. The authors alone are responsible for the content and writing of the paper.

Downloaded By: [Kyushu University Central Library] At: 03:45 11 May 2009

References

[1] Gheorghiade M, Bonow RO. Chronic heart failure in the United States: a manifestation of coronary artery disease. Circulation 1998;97:282–289.

[2] Cohn JN, Ferrari R, Sharpe N. Cardiac remodeling—concepts and clinical implications: a consensus paper from an international forum on cardiac remodeling. Behalf of an International Forum on Cardiac Remodeling. J Am Coll Cardiol 2000;35:569–582.

[3] Liew CC, Dzau VJ. Molecular genetics and genomics of heart failure. Nat Rev Genet 2004;5:811–825.

[4] Tsutsui H, Ide T, Hayashidani S, Kinugawa S, Suematsu N, Utsumi H, Takeshita A. Effects of ACE inhibition on left ventricular failure and oxidative stress in Dahl salt-sensitive rats. J Cardiovasc Pharmacol 2001;37:725–733.

[5] Ichihara S, Yamada Y, Ichihara G, Kanazawa H, Hashimoto K, Kato Y, Matsushita A, Oikawa S, Yokota M, Iwase M. Attenuation of oxidative stress and cardiac dysfunction by bisoprolol in an animal model of dilated cardiomyopathy. Biochem Biophys Res Commun 2006;350:105–113.

[6] Mollnau H, Oelze M, August M, Wendt M, Daiber A, Schulz E, Baldus S, Kleschyov AL, Materne A, Wenzel P, Hink U, Nickenig G, Fleming I, Munzel T. Mechanisms of increased vascular superoxide production in an experimental model of idiopathic dilated cardiomyopathy. Arterioscler Thromb Vasc Biol 2005;25:2554–2559.

[7] Shite J, Qin F, Mao W, Kawai H, Stevens SY, Liang C. Antioxidant vitamins attenuate oxidative stress and cardiac dysfunction in tachycardia-induced cardiomyopathy. J Am Coll Cardiol 2001;38:1734–1740.

[8] Carlberg I, Mannervik B. Purification and characterization of the flavoenzyme glutathione reductase from rat liver. J Biol Chem 1975;250:5475–5480.

[9] Ide T, Tsutsui H, Kinugawa S, Suematsu N, Hayashidani S, Ichikawa K, Utsumi H, Machida Y, Egashira K, Takeshita A. Direct evidence for increased hydroxyl radicals originating from superoxide in the failing myocardium. Circ Res 2000;86:152–157.

[10] Lang D, Mosfer SI, Shakesby A, Donaldson F, Lewis MJ. Coronary microvascular endothelial cell redox state in left ventricular hypertrophy: the role of angiotensin II. Circ Res 2000;86:463–469.

[11] Kinugawa S, Tsutsui H, Hayashidani S, Ide T, Suematsu N, Satoh S, Utsumi H, Takeshita A. Treatment with dimethylthiourea prevents left ventricular remodeling and failure after experimental myocardial infarction in mice: role of oxidative stress. Circ Res 2000;87:392–398.

[12] Shiomi T, Tsutsui H, Matsusaka H, Murakami K, Hayashidani S, Ikeuchi M, Wen J, Kubota T, Utsumi H, Takeshita A. Overexpression of glutathione peroxidase prevents left ventricular remodeling and failure after myocardial infarction in mice. Circulation 2004;109:544–549.

[13] Matsushima S, Kinugawa S, Ide T, Matsusaka H, Inoue N, Ohta Y, Yokota T, Sunagawa K, Tsutsui H. Overexpression of glutathione peroxidase attenuates myocardial remodeling and preserves diastolic function in diabetic heart. Am J Physiol Heart Circ Physiol 2006;291:H2237–H2245.

[14] Suematsu N, Tsutsui H, Wen J, Kang D, Ikeuchi M, Ide T, Hayashidani S, Shiomi T, Kubota T, Hamasaki N, Takeshita A. Oxidative stress mediates tumor necrosis factor-alpha-induced mitochondrial DNA damage and dysfunction in cardiac myocytes. Circulation 2003;107:1418–1423.

[15] Machida Y, Kubota T, Kawamura N, Funakoshi H, Ide T, Utsumi H, Li YY, Feldman AM, Tsutsui H, Shimokawa H, Takeshita A. Overexpression of tumor necrosis factor-alpha increases production of hydroxyl radical in murine myocardium. Am J Physiol Heart Circ Physiol 2003;284:H449–H455.

[16] Foo RS, Siow RC, Brown MJ, Bennett MR. Heme oxygenase-1 gene transfer inhibits angiotensin II-mediated rat cardiac myocyte apoptosis but not hypertrophy. J Cell Physiol 2006;209:1–7.

[17] Nakagami H, Takemoto M, Liao JK. NADPH oxidase-derived superoxide anion mediates angiotensin II-induced cardiac hypertrophy. J Mol Cell Cardiol 2003;35:851–859.

[18] Siwik DA, Chang DL, Colucci WS. Interleukin-1beta and tumor necrosis factor-alpha decrease collagen synthesis and increase matrix metalloproteinase activity in cardiac fibroblasts *in vitro*. Circ Res 2000;86:1259–1265.

[19] Siwik DA, Pagano PJ, Colucci WS. Oxidative stress regulates collagen synthesis and matrix metalloproteinase activity in cardiac fibroblasts. Am J Physiol Cell Physiol 2001;280:C53–C60.

[20] Matsushima S, Ide T, Yamato M, Matsusaka H, Hattori F, Ikeuchi M, Kubota T, Sunagawa K, Hasegawa Y, Kurihara T, Oikawa S, Kinugawa S, Tsutsui H. Overexpression of mitochondrial peroxiredoxin-3 prevents left ventricular remodeling and failure after myocardial infarction in mice. Circulation 2006;113:1779–1786.

[21] Pimentel DR, Amin JK, Xiao L, Miller T, Viereck J, Oliver-Krasinski J, Baliga R, Wang J, Siwik DA, Singh K, Pagano P, Colucci WS, Sawyer DB. Reactive oxygen species mediate amplitude-dependent hypertrophic and apoptotic responses to mechanical stretch in cardiac myocytes. Circ Res 2001;89:453–460.

[22] Shiomi T, Tsutsui H, Hayashidani S, Suematsu N, Ikeuchi M, Wen J, Ishibashi M, Kubota T, Egashira K, Takeshita A. Pioglitazone, a peroxisome proliferator-activated receptor-gamma agonist, attenuates left ventricular remodeling and failure after experimental myocardial infarction. Circulation 2002;106:3126–3132.

[23] Yamamoto Y, Takahashi K. Glutathione peroxidase isolated from plasma reduces phospholipid hydroperoxides. Arch Biochem Biophys 1993;305:541–545.

[24] Sano H, Matsumoto K, Utsumi H. Synthesis and imaging of blood-brain-barrier permeable nitroxyl-probes for free radical reactions in brain of living mice. Biochem Mol Biol Int 1997;42:641–647.

[25] Han JY, Takeshita K, Utsumi H. Noninvasive detection of hydroxyl radical generation in lung by diesel exhaust particles. Free Radic Biol Med 2001;30:516–525.

[26] Phumala N, Ide T, Utsumi H. Noninvasive evaluation of *in vivo* free radical reactions catalyzed by iron using *in vivo* ESR spectroscopy. Free Radic Biol Med 1999;26:1209–1217.
[27] Belch JJ, Bridges AB, Scott N, Chopra M. Oxygen free radicals and congestive heart failure. Br Heart J 1991;65:245–248.
[28] Dieterich S, Bieligk U, Beulich K, Hasenfuss G, Prestle J. Gene expression of antioxidative enzymes in the human heart: increased expression of catalase in the end-stage failing heart. Circulation 2000;101:33–39.
[29] Ide T, Tsutsui H, Hayashidani S, Kang D, Suematsu N, Nakamura K, Utsumi H, Hamasaki N, Takeshita A. Mitochondrial DNA damage and dysfunction associated with oxidative stress in failing hearts after myocardial infarction. Circ Res 2001;88:529–535.
[30] Cargnoni A, Ceconi C, Bernocchi P, Boraso A, Parrinello G, Curello S, Ferrari R. Reduction of oxidative stress by carvedilol: role in maintenance of ischaemic myocardium viability. Cardiovasc Res 2000;47:556–566.
[31] Guo P, Nishiyama A, Rahman M, Nagai Y, Noma T, Namba T, Ishizawa M, Murakami K, Miyatake A, Kimura S, Mizushige K, Abe Y, Ohmori K, Kohno M. Contribution of reactive oxygen species to the pathogenesis of left ventricular failure in Dahl salt-sensitive hypertensive rats: effects of angiotensin II blockade. J Hypertens 2006;24:1097–1104.
[32] Miwa S, Toyokuni S, Nishina T, Nomoto T, Hiroyasu M, Nishimura K, Komeda M. Spaciotemporal alteration of 8-hydroxy-2′-deoxyguanosine levels in cardiomyocytes after myocardial infarction in rats. Free Radic Res 2002;36:853–858.
[33] Zhang GX, Kimura S, Nishiyama A, Shokoji T, Rahman M, Yao L, Nagai Y, Fujisawa Y, Miyatake A, Abe Y. Cardiac oxidative stress in acute and chronic isoproterenol-infused rats. Cardiovasc Res 2005;65:230–238.
[34] Li H, Lawson JA, Reilly M, Adiyaman M, Hwang SW, Rokach J, FitzGerald GA. Quantitative high performance liquid chromatography/tandem mass spectrometric analysis of the four classes of F(2)-isoprostanes in human urine. Proc Natl Acad Sci USA 1999;96:13381–13386.
[35] Agnoletti L, Curello S, Bachetti T, Malacarne F, Gaia G, Comini L, Volterrani M, Bonetti P, Parrinello G, Cadei M, Grigolato PG, Ferrari R. Serum from patients with severe heart failure downregulates eNOS and is proapoptotic: role of tumor necrosis factor-alpha. Circulation 1999;100:1983–1991.
[36] Kunsch C, Medford RM. Oxidative stress as a regulator of gene expression in the vasculature. Circ Res 1999;85:753–766.
[37] Al-Mehdi AB, Zhao G, Dodia C, Tozawa K, Costa K, Muzykantov V, Ross C, Blecha F, Dinauer M, Fisher AB. Endothelial NADPH oxidase as the source of oxidants in lungs exposed to ischemia or high K+. Circ Res 1998;83:730–737.
[38] Iuchi T, Akaike M, Mitsui T, Ohshima Y, Shintani Y, Azuma H, Matsumoto T. Glucocorticoid excess induces superoxide production in vascular endothelial cells and elicits vascular endothelial dysfunction. Circ Res 2003;92:81–87.
[39] Bertuglia S, Giusti A. Microvascular oxygenation, oxidative stress, NO suppression and superoxide dismutase during postischemic reperfusion. Am J Physiol Heart Circ Physiol 2003;285:H1064–H1071.
[40] Taniyama Y, Griendling KK. Reactive oxygen species in the vasculature: molecular and cellular mechanisms. Hypertension 2003;42:1075–1081.
[41] Aebi H. Catalase *in vitro*. Methods Enzymol 1984;105:121–126.
[42] Nakamura H, Takata S, Umemoto S, Matsuzaki M. Induction of left ventricular remodeling and dysfunction in the recipient heart following donor heart myocardial infarction: new insights into the pathological role of tumor necrosis factor-alpha from a novel heterotopic transplant-coronary ligation model. J Cardiol 2003;41:41–42.
[43] Maury CP. Monitoring the acute phase response: comparison of tumour necrosis factor (cachectin) and C-reactive protein responses in inflammatory and infectious diseases. J Clin Pathol 1989;42:1078–1082.
[44] Guillen I, Blanes M, Gomez-Lechon MJ, Castell JV. Cytokine signaling during myocardial infarction: sequential appearance of IL-1 beta and IL-6. Am J Physiol 1995;269:R229–R235.
[45] Basaran Y, Basaran MM, Babacan KF, Ener B, Okay T, Gok H, Ozdemir M. Serum tumor necrosis factor levels in acute myocardial infarction and unstable angina pectoris. Angiology 1993;44:332–337.
[46] Marx N, Neumann FJ, Ott I, Gawaz M, Koch W, Pinkau T, Schomig A. Induction of cytokine expression in leukocytes in acute myocardial infarction. J Am Coll Cardiol 1997;30:165–170.
[47] Fine PE. Implications of different study designs for the evaluation of acellular pertussis vaccines. Dev Biol Stand 1997;89:123–133.
[48] Pratico D, Lawson JA, Rokach J, FitzGerald GA. The isoprostanes in biology and medicine. Trends Endocrinol Metab 2001;12:243–247.

This paper was first published online on iFirst on 1 December 2008.

Downloaded By: [Kyushu University Central Library] At: 03:45 11 May 2009

Annals of Biomedical Engineering, Vol. 37, No. 1, January 2009 (© 2008) pp. 82–93
DOI: 10.1007/s10439-008-9595-8

Computationally Managed Bradycardia Improved Cardiac Energetics While Restoring Normal Hemodynamics in Heart Failure

KAZUNORI UEMURA,[1] KENJI SUNAGAWA,[2] and MASARU SUGIMACHI[1]

[1]Department of Cardiovascular Dynamics, Advanced Medical Engineering Center, National Cardiovascular Center Research Institute, 5-7-1 Fujishirodai, Suita 565-8565, Japan; and [2]Department of Cardiovascular Medicine, Kyushu University Graduate School of Medical Sciences, Fukuoka 812-8582, Japan

(*Received 9 September 2008; accepted 29 October 2008; published online 12 November 2008*)

Abstract—In acute heart failure, systemic arterial pressure (AP), cardiac output (CO), and left atrial pressure (P_{LA}) have to be controlled within acceptable ranges. Under this condition, cardiac energetic efficiency should also be improved. Theoretically, if heart rate (HR) is reduced while AP, CO, and P_{LA} are maintained by preserving the functional slope of left ventricular (LV) Starling's curve (S_L) with precisely increased LV end-systolic elastance (E_{es}), it is possible to improve cardiac energetic efficiency and reduce LV oxygen consumption per minute (MVO_2). We investigated whether this hemodynamics can be accomplished in acute heart failure using an automated hemodynamic regulator that we developed previously. In seven anesthetized dogs with acute heart failure ($CO < 70$ mL min^{-1} kg^{-1}, $P_{LA} > 15$ mmHg), the regulator simultaneously controlled S_L with dobutamine, systemic vascular resistance with nitroprusside and stressed blood volume with dextran or furosemide, thereby controlling AP, CO, and P_{LA}. Normal hemodynamics were restored and maintained (CO; 88 ± 3 mL min^{-1} kg^{-1}, P_{LA}; 10.9 ± 0.4 mmHg), even when zatebradine significantly reduced HR (−27 ± 3%). Following HR reduction, E_{es} increased (+34 ± 14%), LV mechanical efficiency (stroke work/oxygen consumption) increased (+22 ± 6%), and MVO_2 decreased (−17 ± 4%) significantly. In conclusion, in a canine acute heart failure model, computationally managed bradycardia improved cardiac energetic efficiency while restoring normal hemodynamic conditions.

Keywords—Ventricular oxygen consumption, Mechanical efficiency, Specific bradycardic agent.

INTRODUCTION

Systemic arterial pressure (AP), cardiac output (CO), and left atrial pressure (P_{LA}) are three major variables necessary to guarantee survival. In the management of patients with acute heart failure following myocardial infarction or cardiac surgery, these variables have to be controlled within acceptable ranges.[1] Since the failing heart is in a critical state of myocardial energetics,[19] improvement of cardiac energetic efficiency is also essential in the management of such patients. Therapeutic interventions that enhance cardiac energetic efficiency have proven to be beneficial with respect to long-term outcome.[20] Reduction of heart rate (HR) has been shown to improve cardiac energetic efficiency.[6,26] However, in the failing heart, reduction of HR alone may decrease CO, and compromise hemodynamics.[5,13]

We previously demonstrated that AP, CO, and P_{LA} are determined by a mechanical equilibrium of the functional slope of Starling's curve (S_L) for the left ventricle (LV), systemic vascular resistance (R), and stressed blood volume (V).[30–32] Conversely, S_L, R, and V can be calculated from AP, CO, and P_{LA}, indicating that a set of AP, CO, and P_{LA} values uniquely corresponds to a set of S_L, R, and V values. When HR is reduced, the three variables of AP, CO, and P_{LA} can only be maintained by increasing LV contractility (LV end-systolic elastance, E_{es}) to offset HR reduction and to preserve S_L (see *Theoretical analysis* in "Materials and Methods"). In this hemodynamics, total mechanical energy of LV contraction, which is indicated by LV pressure–volume area (PVA), also increases with HR reduction. Increases in both E_{es} and PVA elevate LV oxygen consumption per beat (BVO_2).[28,29] However, since the increase in the external work done by LV is greater than the increase in BVO_2, cardiac energetic efficiency is improved. Furthermore, LV oxygen consumption per minute (MVO_2) decreases because the reduction in HR is sufficient to compensate for the increase in BVO_2.

To realize the above hemodynamics (optimal hemodynamics) in patients with acute heart failure, AP, CO, and P_{LA} should be controlled under HR

Address correspondence to Kazunori Uemura, Department of Cardiovascular Dynamics, Advanced Medical Engineering Center, National Cardiovascular Center Research Institute, 5-7-1 Fujishirodai, Suita 565-8565, Japan. Electronic mail: kuemura@ri.ncvc.go.jp

0090-6964/09/0100-0082/0 © 2008 Biomedical Engineering Society

reduction by regulating infusions of multiple cardiovascular drugs such as inotropes and vasodilators. However, the control process is difficult and time-consuming, since the responses of AP, CO, and P_{LA} to these drugs vary between patients and within patient over time, and the responses are interrelated.[9,23] We previously demonstrated that it is possible to control AP, CO, and P_{LA} stably and accurately by directly controlling S_L, R, and V with cardiovascular drugs, due to their mechanical equilibrium.[30] This strategy is feasible because the responses of S_L to inotropes, R to vasodilators, and V to volume expander or diuretics are relatively invariable.[30] Furthermore, these three input–output relations; namely, inotrope–S_L, vasodilator–R, and volume expanders/diuretics–V are effectively decoupled. We hypothesized that this approach would be especially efficacious in accomplishing optimal hemodynamics in acute heart failure. Under HR reduction, an excessive increase in E_{es} will compromise the cardiac energetic efficiency.[15] Therefore E_{es} should be increased to a precise level. This can be done through a tight control of the inotrope–S_L relation. Although inotropes also affect R or V,[3,7] these effects can easily be compensated by the vasodilator–R and volume expanders/diuretics–V relations.

The purpose of this study was to prove the hypothesis that direct control of S_L, R, and V under HR reduction attains the optimal hemodynamics and at the same time improves cardiac energetic efficiency and reduces MVO_2 in a canine model of acute heart failure, as predicted in *Theoretical Analysis*. An automated hemodynamic regulator that we developed previously[30] was used to directly control S_L, R, and V. The regulator directly controls S_L with dobutamine (DOB), R with sodium nitroprusside (SNP), and V with dextran (DEX) and furosemide (FUR), thereby controlling AP, CO, and P_{LA}. To reduce HR, we used a specific bradycardic agent, zatebradine (UL-FS49) that specifically reduces HR without affecting LV contractility.[12,24]

MATERIALS AND METHODS

Theoretical analysis

S_L is theoretically determined by E_{es}, HR, R, and diastolic myocardial stiffness (k), and can be expressed by the following formula[31]:

$$S_L = \frac{1}{k} \cdot \frac{E_{es}}{(E_{es}/HR) + R} \tag{1}$$

Equation (1) can be rewritten as follows:

$$E_{es} = \frac{S_L \cdot k \cdot R}{1 - S_L \cdot k/HR} \tag{2}$$

The external work done by LV is represented by stroke work (SW) and expressed as[11]

$$SW = (P_{es} - P_{ed}) \cdot CO/HR \tag{3}$$

where P_{es} is LV end-systolic pressure and P_{ed} is end-diastolic pressure. In the LV pressure–volume diagram, PVA is the area circumscribed by the end-systolic pressure volume relation, the end-diastolic pressure volume relation, and the systolic pressure volume trajectory of LV. PVA, an index of total mechanical energy of LV contraction, is the sum of potential energy and external work of LV,[28,29] and can be expressed as

$$PVA = P_{es} \cdot P_{es}/2E_{es} + SW \tag{4}$$

If we approximate P_{es} to AP and P_{ed} to P_{LA}, SW and PVA can be expressed as

$$SW = (AP - P_{LA}) \cdot CO/HR \tag{5}$$

$$PVA = AP \cdot AP/2E_{es} + SW \tag{6}$$

BVO_2 is related to PVA and E_{es} as follows[28,29]:

$$BVO_2 = \alpha \cdot PVA + \beta \cdot E_{es} + \gamma \tag{7}$$

where α, β, and γ are constants representing oxygen cost of PVA, oxygen cost of contractility, and basal metabolism, respectively. MVO_2 is expressed as follows:

$$MVO_2 = BVO_2 \cdot HR \tag{8}$$

Using Eqs. (2–8) and fixed values of AP, CO, and P_{LA} (Table 1), we numerically simulated the individual relations of HR with E_{es}, SW, PVA, BVO_2, LV mechanical efficiency (ME) and MVO_2 (Fig. 1). In these computations, representative k, α, β, and γ values (Table 1) were used, which are appropriate for a 20-kg dog.[10,29] In Eq. (2), S_L was calculated from the ratio of CO to logarithmic function of P_{LA} as described

TABLE 1. Values of the parameters used in *Theoretical Analysis*.

Parameters	Values
AP, mmHg	100
CO, mL min^{-1} kg^{-1}	100
P_{LA}, mmHg	10
k, mL^{-1}	0.082
α, mL O_2 · $mmHg^{-1}$ · mL^{-1}	1.8×10^{-5}
β, mL O_2 · $beat^{-1}$ · $mmHg^{-1}$ · mL	0.0018
γ, mL O_2 · $beat^{-1}$	0.01

AP, systemic arterial pressure; CO, cardiac output; P_{LA}, left atrial pressure; k, left ventricular diastolic myocardial stiffness; α, oxygen cost of pressure–volume area; β, oxygen cost of contractility; γ, constant representing basal metabolism.

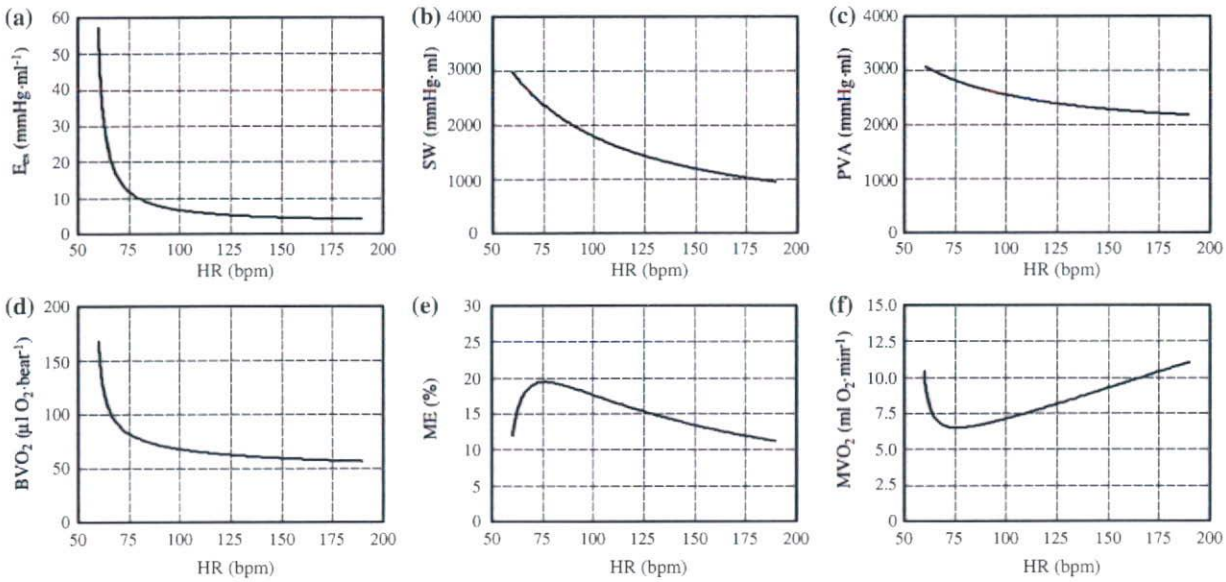

FIGURE 1. Simulated relations of heart rate (*HR*) with left ventricular end-systolic elastance (E_{es}) (a), left ventricular stroke work (*SW*) (b), left ventricular pressure–volume area (*PVA*) (c), left ventricular oxygen consumption per beat (BVO_2) (d), left ventricular mechanical efficiency (*ME*) (e), and left ventricular oxygen consumption per minute (MVO_2) (f), when systemic arterial pressure, cardiac output, and left atrial pressure are kept at fixed values. At *HR* of 75 bpm, *ME* becomes maximal (e), and MVO_2 becomes minimal (f).

previously.[30] R was calculated from the ratio of AP to CO. ME was calculated as the dimensionless ratio of SW to BVO_2.[19]

As indicated in Fig. 1, HR is inversely related to E_{es} (Fig. 1a), SW (Fig. 1b), PVA (Fig. 1c), and BVO_2 (Fig. 1d). Over the physiological range of HR for dogs (>80 bpm),[18] ME increases as HR is reduced (Fig. 1e) since SW increase is greater than BVO_2 increase; hence cardiac energetic efficiency is optimized. At HR of 75 bpm, ME becomes maximal and MVO_2 becomes minimal (Fig. 1f). When HR is reduced from 150 to 110 bpm, E_{es} increases from 4.6 to 5.9 mmHg mL^{-1} (29% increase) and ME increases from 13 to 17% (24% increase), whereas MVO_2 decreases from 8.9 to 7.2 mL O_2 min^{-1} (19% reduction). In addition to the simulation described above, we also simulated the relation of HR with MVO_2 for a variety of combinations of AP (80–120 mmHg), CO (80–100 mL min^{-1} kg^{-1}), and P_{LA} (10–20 mmHg). HR at which MVO_2 becomes minimal ranged from 50 to 75 bpm (data not shown). This indicates that as long as HR is within the physiological range, HR reduction together with compensatory increase of E_{es} consistently improves cardiac energetic efficiency and reduces MVO_2, irrespective of the target hemodynamics to be achieved.

Animal Preparation

After approval of the institutional Animal Care and Use Committee we studied 7 adult mongrel dogs (either sexes, 26 ± 4 kg). Anesthesia was induced with sodium pentobarbital (25 mg kg^{-1}). Animals were intubated endotracheally. Arterial pH, PO_2, and PCO_2 were maintained within the physiological ranges. Isoflurane (1.0%) was inhaled continuously during the experiment. After a median sternotomy and pericardial incision, an ultrasonic flow-meter (20A594, Transonics, Ithaca, NY) was placed around the ascending aorta to measure CO. Ultrasonic flow meters (2.5S273, Transonics, Ithaca, NY) were placed on the left circumflex and anterior descending coronary arteries to measure coronary blood flow. Fluid filled catheters were placed in the right femoral artery, left atrium and right atrium, and connected to pressure transducers (DX-200, Nihon Kohden, Tokyo, Japan) to measure AP, P_{LA}, and right atrial pressure, respectively. A catheter-tipped micromanometer (SPC-330A, Millar Instruments, Houston, TX) was introduced into the left ventricle to measure left ventricular pressure (LVP). A pair of pacing electrodes was fixed at the right atrial appendage for atrial pacing. A catheter (5F) was introduced into the coronary sinus via the right external jugular vein.

Two infusion pumps (CFV-3200, Nihon Kohden, Tokyo, Japan) for administering DOB and SNP, and a roller pump (Minipulse 3, Gilson, Middleton, WI) for administering DEX were attached to a catheter (5F) placed in the right femoral vein. These pumps were controlled with a laboratory computer (MA20V, NEC, Tokyo, Japan). From a catheter (5F) placed in the

right external jugular vein, FUR was injected following a command signal from the computer.

Analog signals of *AP*, *CO*, P_{LA}, right atrial pressure, LVP, and coronary blood flow were digitized (200 Hz, 12-bit) by the computer, and stored on a hard disk for off-line analysis. The digitized signals of *AP*, *CO*, and P_{LA} were smoothed by a low-pass filter with a time constant 10 s, and used as control variables for the regulator.

Automated Hemodynamic Regulator

Figure 2 is a schematic illustration of the automated hemodynamic regulator.[30] Once target values for *AP*, *CO*, and P_{LA} are defined and fed into the computer, it calculates the target values for S_L, *R*, and *V*. The subject's S_L, *R*, and *V* are calculated from the low-pass filtered *AP*, *CO*, and P_{LA} values. To minimize the differences between target and subject's S_L and *R*, proportional-integral feedback controllers adjust the infusion rates of DOB and SNP, respectively. To minimize the difference between target and subject's *V*, a nonlinear feedback controller adjusts the infusion of DEX or injection of FUR (see Appendix: Feedback control algorithms of the automatic hemodynamic regulator).

Experimental Protocols

After stabilization for 30 min, "baseline" hemodynamic data were recorded and blood samples were collected from the right femoral artery and the coronary sinus simultaneously for oxygen content determination (*Baseline*). Acute heart failure was induced by injecting glass microspheres (90 μm in diameter) to embolize the left circumflex coronary artery.[27] The amount of microspheres was adjusted to decrease *CO* to below 70 mL min^{-1} kg^{-1} or increase P_{LA} to above 15 mmHg. One hour after embolization, zatebradine (0.5 mg kg^{-1}) was administered intravenously to suppress the intrinsic atrial beat, and atrial pacing was then initiated to control *HR* at the level observed following coronary embolization. After the canine model of acute heart failure was established, hemodynamic measurements and blood sample collection were performed (*AHF*).

We activated the automated hemodynamic regulator with target values of 90–100 mmHg for *AP*, 80–100 mL kg^{-1} min^{-1} for *CO*, and 10–12 mmHg for P_{LA}. The regulator restored *AP*, *CO*, and P_{LA} to their respective target values within 30 min. After confirming stable hemodynamics, we collected blood samples as described above (*Initial HR*). We then reduced the pacing rate in steps of 10 or 20 bpm. The maximum *HR* reduction averaged 39 ± 12 bpm. For each *HR* step, we waited for hemodynamic stabilization, and then collected blood samples. After reaching the lowest HR (*Lowest HR*), we increased the *HR* stepwise back to the "Initial *HR*" to confirm the reproducibility of the hemodynamic control.

Data Analysis of LV Mechanoenergetics

We estimated E_{es} using a technique described previously.[14] In brief, the ratio of E_{es} to effective arterial elastance was estimated based on the fact that this ratio can be expressed as a function of P_{es}, LVP at which LV begins to eject, pre-ejection period, and

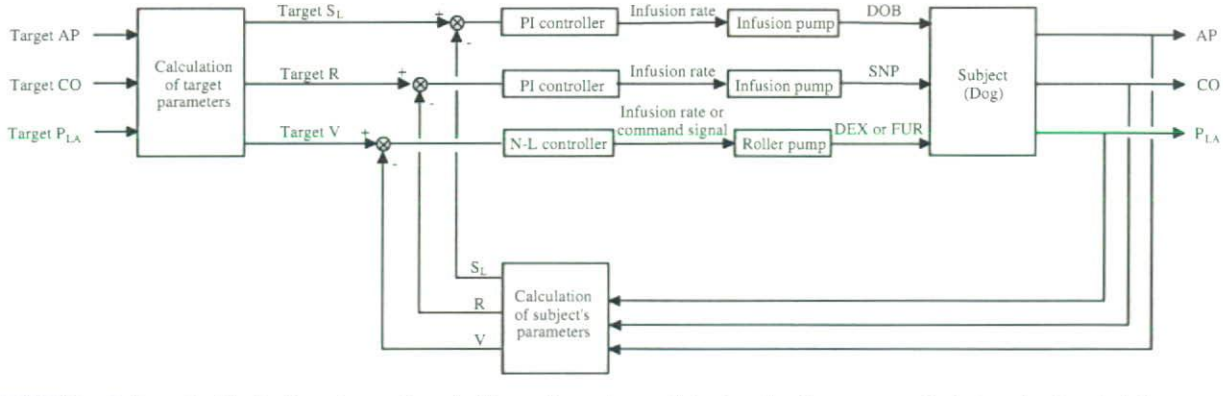

FIGURE 2. Schematic illustration of an automated hemodynamic regulator for simultaneous control of systemic arterial pressure (*AP*), cardiac output (*CO*), and left atrial pressure (P_{LA}). From target values of *AP*, *CO*, and P_{LA}, target values of functional slope of the left ventricular Starling's curve (S_L), systemic vascular resistance (*R*), and stressed blood volume (*V*) are determined. Subject's S_L, *V*, and *R* are calculated from low-pass filtered values of measured *AP*, *CO*, and P_{LA}. Proportional-integral (PI) feedback controllers adjust infusion rate of dobutamine (DOB) and sodium nitroprusside (SNP) to minimize the difference between target and subject's S_L and those of *R*, respectively. Nonlinear (N-L) feedback controller adjusts infusion of 10% dextran 40 (DEX) or injection of furosemide (FUR) to minimize the difference between target and subject's *V*.

ejection time. Effective arterial elastance is calculated as P_{es} divided by stroke volume. Therefore once we know the ratio, we can calculate E_{es}.[14] In this study, the end-diastolic point is defined as the moment when LV dP/dt exceeds 20% of positive dP/dt_{max}. The time point at which LV begins to eject is defined as the moment when the aortic flow begins. The end-systolic point is defined as the time when LV dP/dt decreases to 20% of LV dP/dt_{min}. Thus, pre-ejection period is obtained by subtracting the end-diastolic point from the time point at which LV begins to eject; and ejection time is obtained by subtracting the time point at which LV begins to eject from the end-systolic point.

SW was calculated using Eq. (3). *PVA* was calculated using Eq. (4). Oxygen contents of the blood samples were measured using a co-oxymeter (IL 682, Instrumentation Laboratory, Lexington, MA), and MVO_2 was calculated as the product of mean coronary blood flow and the coronary arteriovenous difference in oxygen content.[6] BVO_2 was calculated by dividing MVO_2 by *HR*. *ME* was calculated as described above.

Statistics

Group data are expressed as means ± SEM. Differences in hemodynamics, LV mechanoenergetics, and drug infusion rates among different conditions were evaluated using Student's paired *t*-test or a repeated-measures analysis of variance followed by Student-Newman–Keuls test. The level of statistical significance was defined as $p < 0.05$.

RESULTS

Hemodynamic and LV mechanoenergetic data at *Baseline* and *AHF* are summarized in Table 2. Coronary embolization nearly halved *CO* from 101 ± 5 to 62 ± 5 mL min^{-1} kg^{-1}, doubled P_{LA} from 8.9 ± 0.6 to 17.1 ± 0.7 mmHg, depressed E_{es} from 4.4 ± 0.7 to 2.5 ± 0.4 mmHg mL^{-1}, and halved MVO_2 from 5.8 ± 0.7 to 3.1 ± 0.2 mL min^{-1}. These changes are compatible with induction of acute ischemic heart failure.[27]

Figure 3 demonstrates the time courses of hemodynamics, the infusion rates of DOB and SNP, and the infused volume of DEX in a representative animal. Before activation of the regulator, *AP* was 108 mmHg, *CO* was 44 mL min^{-1} kg^{-1}, and P_{LA} was 16.9 mmHg. After activation of the regulator, the infusion rates of DOB, SNP, and DEX were adjusted automatically and S_L, *R*, and *V* reached their respective target values within 20 min. In this case, FUR was not used. By controlling S_L, *R*, and *V*, the regulator restored *AP*, *CO*, and P_{LA} to their respective target values (*AP*, 100 mmHg; *CO*, 80 mL min^{-1} kg^{-1}; P_{LA}, 10 mmHg). After attaining the target values at around 20 min, *AP*, *CO*, and P_{LA} were maintained at these levels stably throughout stepwise changes in *HR*. *HR* was reduced from 130 to 80 bpm in 10-bpm steps. Following *HR* reduction, the regulator increased the infusion rate of DOB to maintain S_L (Fig. 3). The regulator also decreased the infusion rate of SNP, and discontinued DEX infusion, thereby maintaining *R* and *V*, respectively. After attaining the lowest *HR* (80 bpm), *HR* was increased to 100 and 130 bpm. For each *HR* step, *AP*, *CO*, and P_{LA} were precisely controlled with minimum absolute errors from target values (error in *AP*, 3 ± 1 mmHg; error in CO, 1 ± 0 mL min^{-1} · kg^{-1}; error in P_{LA}, 0.3 ± 0.1 mmHg).

TABLE 2. Hemodynamic and left ventricular mechanoenergetic data at baseline (*Baseline*), and after coronary artery embolization (*AHF*).

	Baseline	*AHF*
HR, bpm	140 ± 7	146 ± 8
AP, mmHg	114 ± 4	97 ± 5†
CO, mL min^{-1} · kg^{-1}	101 ± 5	62 ± 5†
P_{LA}, mmHg	8.9 ± 0.6	17.1 ± 0.7†
E_{es}, mmHg mL^{-1}	4.4 ± 0.7	2.5 ± 0.4*
SW, mmHg mL	1667 ± 300	933 ± 91
PVA, mmHg mL	3292 ± 302	3235 ± 515
BVO_2, μL O_2 · beat^{-1}	41 ± 5	21 ± 1†
ME, %	36 ± 4	31 ± 4
MVO_2, mL O_2 · min^{-1}	5.8 ± 0.7	3.1 ± 0.2*

*$p < 0.05$, †$p < 0.01$ vs. *Baseline*. Values are mean ± SEM. *HR*, heart rate; *AP*, systemic arterial pressure; *CO*, cardiac output; P_{LA}, left atrial pressure; E_{es}, left ventricular (LV) end-systolic elastance; *SW*, LV stroke work; *PVA*, LV pressure–volume area; BVO_2, LV oxygen consumption per beat; *ME*, **LV mechanical efficiency;** MVO_2, LV oxygen consumption per minute.

Figure 4 demonstrates the relations of *HR* with E_{es} (Panel a), with *SW* (Panel b), with *PVA* (Panel c), with BVO_2 (Panel d), with *ME* (Panel e), and with MVO_2 (Panel f), which were determined at each *HR* step as shown in Fig. 3. E_{es} paralleled the infusion rate of DOB; the value increased from 2.9 to 5.3 mmHg mL^{-1} with *HR* reduction from 130 to 80 mmHg, and decreased to 3.3 mmHg mL^{-1} following the recovery of *HR* to 130 mmHg (Fig. 4a). *SW*, *PVA*, and BVO_2 increased with *HR* reduction, and decreased following the recovery of *HR* (Figs. 4b–d). Following *HR* reduction, since *SW* increased (+46%) to a greater extent than BVO_2 (+10%), *ME* increased from 51 to 67%. Following the recovery of *HR*, *ME* decreased to 52% (Fig. 4e). MVO_2 decreased from 3.3 to 2.3 mL O_2 min^{-1} with *HR* reduction, and increased to 3.0 mL O_2 min^{-1} following the recovery of *HR* (Fig. 4f). These changes in LV mechanoenergetic data are reasonably compatible with those predicted in *Theoretical analysis* (Fig. 1 compared with Fig. 4).

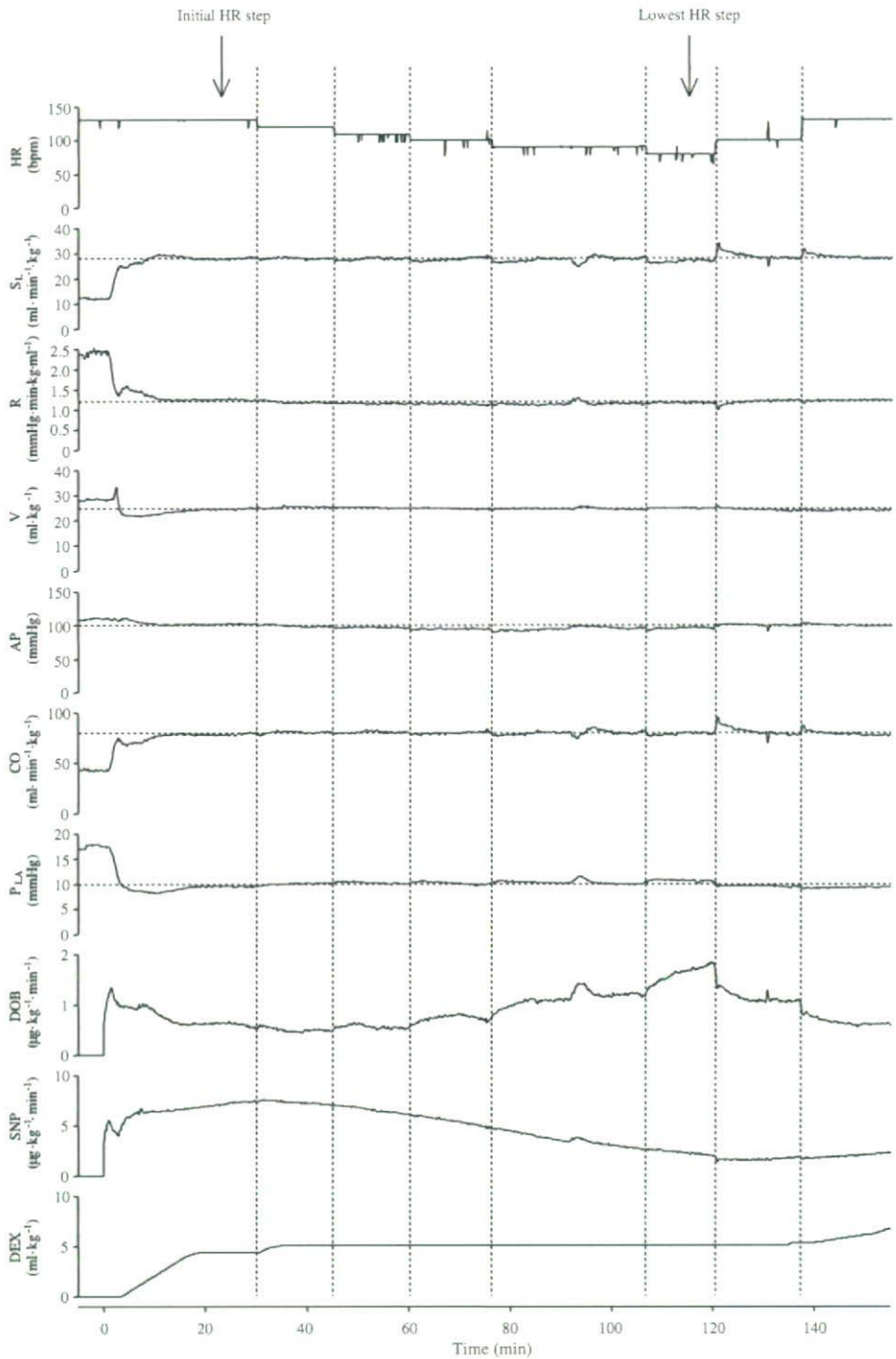

FIGURE 3. Time courses of heart rate (*HR*), S_L, *R*, *V*, *AP*, *CO*, P_{LA}, infusion rates of DOB, SNP, and accumulated volume of infused DEX in one representative animal during control of hemodynamics by the automated hemodynamic regulator. Target values of S_L, *R*, *V*, *AP*, *CO*, and P_{LA} are depicted by horizontal dotted lines in each trace. The *HR* steps (80–130 bpm) are separated by vertical dotted lines.

Table 3 summarizes the hemodynamic and drug infusion data at *AHF*, *Initial HR*, and *Lowest HR* in seven animals. In four animals, FUR (10 mg) was injected once between the *Initial HR* step and the *Lowest HR* step, and the total urine volume was 190–460 mL. Comparing the data at *Initial HR* and

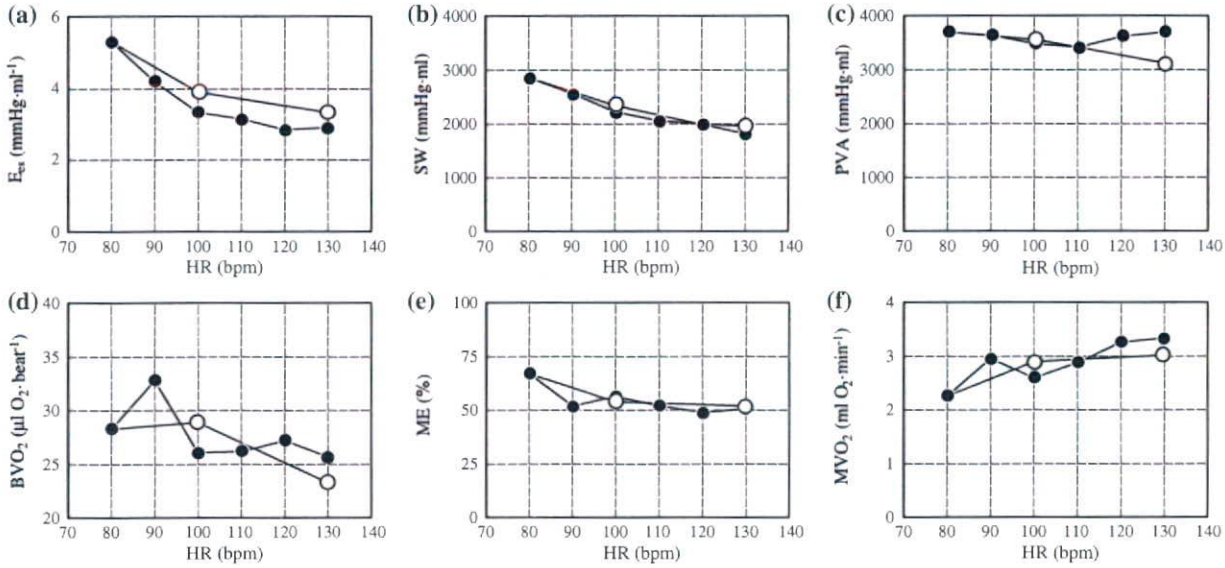

FIGURE 4. Relations of heart rate (*HR*) with left ventricular end-systolic elastance (E_{es}) (a), left ventricular stroke work (*SW*) (b), left ventricular pressure–volume area (*PVA*) (c), left ventricular oxygen consumption per beat (BVO_2) (d), left ventricular mechanical efficiency (*ME*) (e), and left ventricular oxygen consumption per minute (MVO_2) (f) determined at each *HR* step depicted in Fig. 3. •, measurement at each *HR* step while *HR* was reduced from 130 to 80 bpm; ○, measurement at each *HR* step when *HR* was increased from 100 to 130 bpm.

TABLE 3. Hemodynamic data and drug infusion rates after coronary artery embolization (*AHF*), at the initial *HR* (*Initial HR*), and at the lowest *HR* (*Lowest HR*).

	AHF	*Initial HR*	*Lowest HR*
HR, bpm	146 ± 8	146 ± 8	107 ± 7*,†
S_L, mL min^{-1} · kg^{-1}	18 ± 2	31 ± 1*	30 ± 1*
R, mmHg·min · kg · mL^{-1}	1.5 ± 0.2	1.0 ± 0.1*	1.0 ± 0.0*
V, mL · kg^{-1}	31 ± 1	27 ± 1*	27 ± 1*
DOB, µg min^{-1} kg^{-1}		1.4 ± 0.3	2.7 ± 0.5†
SNP, µg min^{-1} kg^{-1}		4.1 ± 0.8	2.4 ± 0.6
DEX, mL kg^{-1}		4.0 ± 0.7	0.8 ± 0.3†
AP, mmHg	97 ± 5	94 ± 3	93 ± 2
CO, mL min^{-1} kg^{-1}	62 ± 5	89 ± 3*	88 ± 3*
P_{LA}, mmHg	17.1 ± 0.7	10.5 ± 0.4*	10.9 ± 0.4*

*$p < 0.01$ vs. *AHF*, †$p < 0.01$ vs. *Initial HR*. Values are mean ± SEM. S_L, functional slope of the left ventricular Starling's curve; *R*, systemic vascular resistance; *V*, stressed blood volume; DOB, infusion rate of dobutamine; SNP, infusion rate of sodium nitroprusside; DEX, the value at *Initial HR* indicates the volume of dextran infused from the activation of the regulator until the *Initial HR*, the value at *Lowest HR* that from the *Initial HR* until the *Lowest HR*.

Lowest HR with those at *AHF*, S_L was increased while *R* and *V* were decreased significantly, indicating that cardiac function was improved while peripheral vasoconstriction and volume retention were relieved by our hemodynamic regulator. As a result, *CO* increased and P_{LA} decreased significantly. *AP*, *CO*, and P_{LA} were controlled precisely in all the animals with minimal absolute errors from target values (error in *AP*, 2 ± 0 mmHg; error in *CO*, 2 ± 0 mL min^{-1} kg^{-1}; error in P_{LA}, 0.4 ± 0.0 mmHg). Comparing the data at *Lowest HR* with those at *Initial HR*, HR decreased significantly (−27 ± 3%), the infusion rate of DOB increased significantly (+116 ± 23%), and the infused volume of DEX decreased significantly (−83 ± 7%).

Figure 5 summarizes the LV mechanoenergetic data at *AHF*, *Initial HR*, and *Lowest HR* in seven animals. When the data at *Initial HR* and *Lowest HR* were compared with those at *AHF*, E_{es}, *SW*, BVO_2, and *ME* increased, but *PVA* decreased significantly. MVO_2 at *Initial HR* also increased compared to that at *AHF*, although MVO_2 at *Lowest HR* was almost identical to that at *AHF*. The automated hemodynamic regulator restored normal hemodynamics with increased energy cost at *Initial HR*, but with diminished energy cost at *Lowest HR*. Comparing the data at *Lowest HR* with those at *Initial HR*, E_{es} increased significantly (+34 ± 14%), *SW* increased significantly (+37 ± 6%), and BVO_2 increased significantly (+12 ± 2%). Since *SW* increased to a greater extent than BVO_2, *ME* increased (+22 ± 6%) and MVO_2 decreased significantly (−17 ± 4%). Changes in the LV mechanoenergetic data following *HR* reduction averaged over seven animals are compatible with those predicted in *Theoretical analysis*.

DISCUSSION

To the best of our knowledge, we are the first to succeed in improving cardiac energetics without compromising normal hemodynamic conditions in acute

heart failure. Only by using our automated hemodynamic regulator, induced bradycardia improved cardiac energetic efficiency while restoring and strictly maintaining normal hemodynamic conditions in a canine model of acute heart failure.

Complicated Multiple Drug Infusions

Complicated regulations of multiple drug infusions were required to maintain AP, CO, and P_{LA} during HR reduction. It is difficult and unrealistic to control multiple drug infusions manually in hemodynamically unstable patients after bradycardia is induced.

Equation (1) indicates that HR reduction alone decreases S_L. In response to HR reduction, the negative feedback mechanism of our regulator automatically increases the infusion rate of DOB, which increases LV E_{es} and maintains S_L (Table 3, Fig. 5). An excessive increase in LV E_{es} can offset the MVO_2-decreasing effect of HR reduction. Therefore, the infusion rate of DOB must be precisely controlled. This is especially important when the oxygen cost of contractility is pathologically increased as observed in heart failure, where an oxygen-wasting effect of DOB may become crucial.[15]

DOB may increase V.[3] Our regulator effectively compensates the volume increasing effect of DOB by reducing or discontinuing DEX infusion, or by infusing FUR (Fig. 3, Table 3). DOB may also change R, and usually reduces R.[3] In some cases, the resistance-lowering effect of DOB is compensated by a decrease in infusion rate of SNP (Fig. 3). If these secondary effects of DOB are not adequately compensated, target hemodynamic conditions can no longer be maintained.

Comparison with Previous Hemodynamic Regulators

Apart from our automated hemodynamic regulator, several systems that automate the infusions of multiple cardiovascular drugs to control AP and CO, or AP and pulmonary arterial pressure have been reported.[17,23,33] However, it would be difficult to use these systems to improve the cardiac energetic efficiency. As indicated in *Theoretical analysis*, cardiac energetic efficiency is determined by HR, AP, CO, and P_{LA}. Those previous systems are incomplete for simultaneously control of all these multiple hemodynamic variables. Unstable performance of these systems sometimes results in drastic change of HR. Persistent oscillations of CO occurred following an abrupt increase in HR during automated hemodynamic control by a previously reported system.[23]

Our regulator controls the mechanical determinants of circulation, and as a result achieves target values for hemodynamic variables.[30] Previous systems[17,23,33]

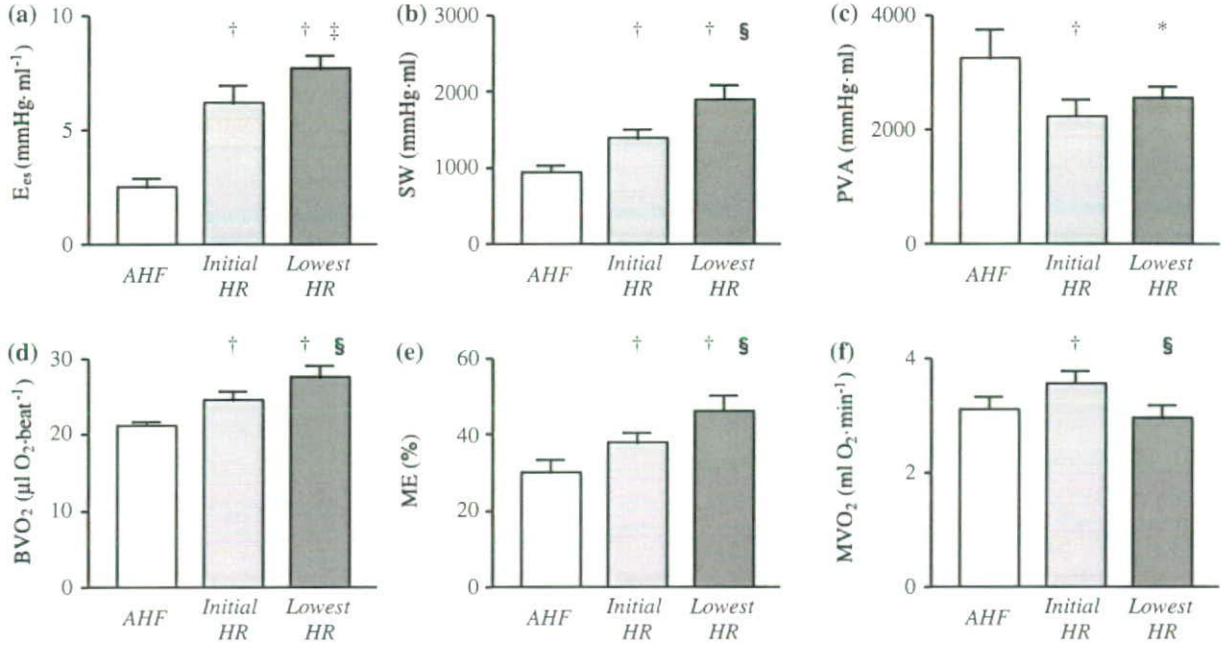

FIGURE 5. Left ventricular mechanoenergetic data after coronary artery embolization (*AHF*), at the initial *HR* (*Initial HR*), and at the lowest *HR* (*Lowest HR*). E_{es}, left ventricular (LV) end-systolic elastance; *SW*, LV stroke work; *PVA*, LV pressure–volume area; BVO_2, LV oxygen consumption per beat; *ME*, **LV mechanical efficiency;** MVO_2, LV oxygen consumption per minute. Data are means ± SEM. $^*p < 0.05$, $^\dagger p < 0.01$ vs. *AHF*. $^\dagger p < 0.05$, $^\S p < 0.01$ vs. *Initial HR*.

attempted to control hemodynamic variables by estimating the apparent input–output relations between drug infusion and response of the controlled variables. In the systems that control *AP* and *CO*,[23,33] all possible input–output relations have to be estimated; namely, inotrope–*AP*, inotrope–*CO*, vasodilator–*AP*, and vasodilator–*CO* relations. The reason is that these drugs affect *AP* and *CO* simultaneously to almost the same degree. If this previous approach is applied to simultaneous control of *AP*, *CO*, and P_{LA}, at least 9 input–output relations have to be estimated, since at least 3 drugs are required to independently control the three variables. This would make the system extremely complicated, and therefore be practically unfeasible. The three drug controllers in our regulator (Fig. 2) are designed on the basis of only three input–output relations between drug infusion and response of the controlled parameter; namely, DOB–S_L, SNP–*R*, and DEX/FUR–*V*.[30] The fact that the three closed loops are effectively decoupled simplifies the entire system. This also permits a system operator, who would be a physician untrained in control engineering, to understand its behavior easily.

Comparison to Previous Studies on LV Mechanoenergetics

Several studies examined LV mechanoenergetics under LV inotropy and bradycardia *in vivo*.[16,25] Single drug or two-drug combinations were used and infusions were titrated manually. However, *HR* reduction inevitably induced changes in *AP*, *CO*, or P_{LA} in these studies.

Shen *et al.*[25] compared the inotropic/chronotropic effects and MVO_2 in response to the sodium channel enhancer LY341311 with those in response to dobutamine in dogs with heart failure. LY341311 increased LV dP/dt_{max} and decreased *HR*. At similar levels of inotropic response and similar levels of *AP* and P_{LA}, dobutamine increased MVO_2 whereas LY341311 did not. These results suggested a favorable effect of LY341311 on myocardial energetics. However, the investigators did not evaluate *CO*. Since left ventricular end-diastolic volume and ventricular fractional shortening were also comparable between the two groups, *CO* must be lower in the LY341311 group in proportion to the magnitude of HR reduction. The favorable effect of LY341311 on myocardial energetics might be in part at the sacrifice of *CO*, i.e., at the sacrifice of peripheral perfusion.

Absolute values of *ME* obtained in the present study (30–70%) were higher than those reported in previous studies (<30%).[19,26,28] Differences in experimental methods may be one reason for this discrepancy. We measured the coronary blood flow using the ultrasonic flow meters placed on the anterior descending and circumflex coronary arteries. However, owing to technical difficulties, blood flow in most proximal branches of the anterior descending artery, such as the first septal and/or first diagonal branches were not included. On the other hand, previous studies using coronary sinus thermo-dilution catheters[19,26] or cross-circulated dog heart preparations[28] were able to measure total coronary artery blood flow including that in proximal branches. Systematic underestimation of coronary blood flow in our study might result in systematic underestimation of ventricular oxygen consumption, and as a result overestimation of *ME*. In addition, *SW* calculated by Eq. (3) does not fully describe the net external work done by LV per cardiac cycle, since diastolic work performed on the ventricle was assessed inaccurately.[11] However, *SW* calculated by Eq. (3) and the net external work determined by the LV pressure–volume loop correlates with high linearity.[11] Taken together, it is fair to say that the direction and magnitude of changes in MVO_2 and *ME* were evaluated accurately in the present study.

Comparison with Beta-blockade Alone

The degree of reduction in MVO_2 (17%, *Lowest HR* vs. *Initial HR* in Fig. 5f) when HR was reduced by 30% in the present experiment is less than that observed in beta-blockade treatment. For example, atenolol decreased MVO_2 by 40% when *HR* was reduced by 30% in dogs during exercise.[6] Negative ventricular inotropy accompanying *HR* reduction accounts for the further reduction in MVO_2 achieved by beta-blockade.[6] However, in acute heart failure, use of beta-blockers is contraindicated owing to its adverse effects on systemic hemodynamics.[1,5] Taken together, the degree of reduction in MVO_2 obtained in this study is reasonable considering that it is achieved without sacrificing the normal hemodynamic condition.

Use of Specific Bradycardic Agent

Under physiological conditions, HR and the ventricular contractility are internally coupled, and is known as the force frequency relationship.[8] In the present study, co-administration of zatebradine with DOB uncoupled this relationship and allowed us to change *HR* and the ventricular contractility (E_{es}) in opposite directions (Fig. 4a).[24] Zatebradine selectively inhibits funny current, which is a primary sinoatrial node pacemaker current, and does not inhibit calcium channel.[12] Therefore, zatebradine reduced *HR* with little influence on the positive inotropic effect of DOB.

Zatebradine has not been further developed for clinical use. Its successor ivabradine belongs to the

same class of selective *HR*-lowering agents that act specifically on the sinoatrial node, and has been approved for clinical application.[4] The fact that ivabradine reduces *HR* dose dependently suggests that in future clinical application of our regulator, we may be able to control the *HR* reduction by titrating ivabradine infusion only without the need of atrial pacing.

Limitations

Figure 1 suggests that if heart rate is reduced beyond a critical value at which MVO_2 becomes minimal, cardiac energetics does not improve, or even deteriorates. This finding indicates that over-reduction of *HR* below the critical value should be avoided when applying the present framework to hemodynamic management. As indicated in Theoretical analysis, satisfactory management would be generally achieved in dogs if *HR* is maintained above 75 bpm. For clinical application of the present framework, a method has to be established to estimate the critical *HR* in each cardiac patient.

We directly measured *CO* and P_{LA} in open chest condition, which is not relevant to the clinical setting. Several methods have been developed to continuously monitor these variables in closed chest conditions.[2] Integrating these methods into our regulator would bring the clinical application of our regulator closer to reality.

The neurohormonal-mediated reflexes, which might have been attenuated by anesthesia in the present study, may cause unstable automated hemodynamic control under conscious condition. Patients with acute heart failure usually have a long history of cardiovascular dysfunction resulting from extensive myocardial remodeling, down-regulation of major receptors controlling HR, contractility, and myocardial oxygen metabolism.[22] This was not the case in our model as the dogs were treated with glass microspheres to induce acute heart failure. Response to our interventional strategy in a chronic heart failure model may be different from that observed in this study. Further studies on these respects are clearly required.

Although reduction in MVO_2 following HR reduction was statistically significant, the degree of reduction was rather mild (Fig. 5f). Furthermore, increase in ventricular contractility suggests that calcium transient may be increased on a single beat basis. Calcium overload closely correlates with myocardial damage and cell death.[21] Whether the improvement in myocardial energetics as achieved in the present study really ameliorates the myocardial damage in acute heart failure remains to be evaluated in future studies.

CONCLUSION

In a canine acute heart failure model, direct control of the mechanical determinants of circulation using an automated hemodynamic regulator improved cardiac energetic efficiency while restoring normal hemodynamic conditions. Our system may be a useful tool in managing hemodynamically unstable patients with acute heart failure.

APPENDIX

Feedback Control Algorithms of the Automatic Hemodynamic Regulator

To minimize the difference between target and subject's S_L (ΔS_L = target S_L—subject's S_L) and those of R (ΔR = target R—subject's R), the proportional-integral (PI) feedback controllers adjust the infusion rates of DOB and SNP, respectively (Fig. 2). In the PI controller (Fig. 6), ΔS_L (or ΔR) and the difference integrated with an integral gain (K_i) are summed and scaled by a proportional gain (K_p) to give the infusion rate of DOB (or SNP). PI gain constants for DOB infusion [$K_i = 0.01\ s^{-1}$, $K_p = 0.06\ \mu g\ kg^{-1}\ min^{-1}$ $(mL\ min^{-1}\ kg^{-1})^{-1}$] and for SNP infusion [$K_i = 0.007\ s^{-1}$, $K_p = -1.37\ \mu g\ kg^{-1}\ min^{-1}$ $(mmHg\ min\ ml^{-1}\ kg)^{-1}$] were determined on the basis of open-loop response of S_L and R to the infusion of DOB and SNP, respectively.[30]

To minimize the difference between target and subject's V (ΔV = target V—subject's V), a nonlinear (N-L) feedback controller (Fig. 2) adjusts the infusion of DEX or injection of FUR based on the following "if-then" rules:

Rule 1: If $\Delta V \geq 1\ mL\ kg^{-1}$ then infuse DEX at $10\ mL\ min^{-1}$
Rule 2: If $\Delta V \leq -2\ mL\ kg^{-1}$ then inject FUR (10 mg) at 10 min intervals

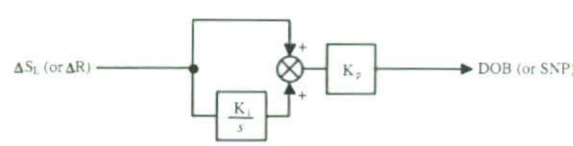

FIGURE 6. Block diagram of the PI controller in the automated hemodynamic regulator. ΔS_L and ΔR denote the difference between target and subject's S_L, and between target and subject's R, respectively. K_i and K_p represent the integral and proportional gain constants, respectively. s is a Laplace operator.

The "if-then" rules were determined on the basis of the open-loop response of V to the infusion of DEX and FUR.[30]

ACKNOWLEDGMENT

This study was supported by Grant-in-Aid for Scientific Research (C) (18500358, 20500404) from the Ministry of Education, Culture, Sports, Science and Technology, by a research grant from Nakatani Foundation of Electronic Measuring Technology Advancement, and by Health and Labour Sciences Research Grants (H19-nano-ippan-009) from the Ministry of Health, Labour and Welfare of Japan.

REFERENCES

[1]Antman, E. M., D. T. Anbe, P. W. Armstrong, E. R. Bates, L. A. Green, M. Hand, J. S. Hochman, H. M. Krumholz, F. G. Kushner, G. A. Lamas, C. J. Mullany, J. P. Ornato, D. L. Pearle, M. A. Sloan, S. C. Smith, Jr., J. S. Alpert, J. L. Anderson, D. P. Faxon, V. Fuster, R. J. Gibbons, G. Gregoratos, J. L. Halperin, L. F. Hiratzka, S. A. Hunt, A. K. Jacobs, and J. P. Ornato. American College of Cardiology; American Heart Association; Canadian Cardiovascular Society ACC/AHA guidelines for the management of patients with ST-elevation myocardial infarction–executive summary. A report of the American College of Cardiology/American Heart Association Task Force on Practice Guidelines (Writing Committee to revise the 1999 guidelines for the management of patients with acute myocardial infarction). *J. Am. Coll. Cardiol.* 44:671–719, 2004. doi:10.1016/j.jacc.2004.07.002.

[2]Bein, B., F. Worthmann, P. H. Tonner, A. Paris, M. Steinfath, and J. Hedderich. Comparison of esophageal Doppler, pulse contour analysis, and real-time pulmonary artery thermodilution for the continuous measurement of cardiac output. *J. Cardiothorac. Vasc. Anesth.* 18:185–189, 2004. doi:10.1053/j.jvca.2004.01.025.

[3]Binkley, P. F., K. D. Murray, K. M. Watson, P. D. Myerowitz, and C. V. Leier. Dobutamine increases cardiac output of the total artificial heart. Implications for vascular contribution of inotropic agents to augmented ventricular function. *Circulation* 84:1210–1215, 1991.

[4]Borer, J. S., K. Fox, P. Jaillon, and G. Lerebours. Antianginal and antiischemic effects of ivabradine, an I(f) inhibitor, in stable angina: a randomized, double-blind, multicentered, placebo-controlled trial. *Circulation* 107: 817–823, 2003. doi:10.1161/01.CIR.0000048143.25023.87.

[5]Choong, C. Y., G. S. Roubin, P. J. Harris, Y. Tokuyasu, W. F. Shen, G. J. Bautovich, and D. T. Kelly. A comparison of the effects of beta-blockers with and without intrinsic sympathomimetic activity on hemodynamics and left ventricular function at rest and during exercise in patients with coronary artery disease. *J. Cardiovasc. Pharmacol.* 8:441–448, 1986. doi:10.1097/00005344-198605000-00001.

[6]Colin, P., B. Ghaleh, X. Monnet, J. Su, L. Hittinger, J. F. Giudicelli, and A. Berdeaux. Contributions of heart rate and contractility to myocardial oxygen balance during exercise. *Am. J. Physiol. Heart Circ. Physiol.* 284:H676–H682, 2003.

[7]Colucci, W. S. Myocardial and vascular actions of milrinone. *Eur. Heart J.* 10(Suppl C):32–38, 1989.

[8]Freeman, G. L., W. C. Little, and R. A. O'Rourke. Influence of heart rate on left ventricular performance in conscious dogs. *Circ. Res.* 61:455–464, 1987.

[9]Gingrich, K. J., and R. J. Roy. Modeling the hemodynamic response to dopamine in acute heart failure. *IEEE Trans. Biomed. Eng.* 38:267–272, 1991. doi:10.1109/10.133208.

[10]Glantz, S. A. Ventricular pressure–volume curve indices change with end-diastolic pressure. *Circ. Res.* 39:772–778, 1976.

[11]Glower, D. D., J. A. Spratt, N. D. Snow, J. S. Kabas, J. W. Davis, C. O. Olsen, G. S. Tyson, D. C. Sabiston, Jr., and J. S. Rankin. Linearity of the Frank–Starling relationship in the intact heart: the concept of preload recruitable stroke work. *Circulation* 71:994–1009, 1985.

[12]Guth, B. D., and T. Dietze. If current mediates β-adrenergic enhancement of heart rate but not contractility in vivo. *Basic Res. Cardiol.* 90:192–202, 1995. doi:10.1007/BF00805662.

[13]Hamlin, R. L., T. Nakayama, H. Nakayama, and C. A. Carnes. Effects of changing heart rate on electrophysiological and hemodynamic function in the dog. *Life Sci.* 72:1919–1930, 2003. doi:10.1016/S0024-3205(03)00015-8.

[14]Hayashi, K., K. Shigemi, T. Shishido, M. Sugimachi, and K. Sunagawa. Single-beat estimation of ventricular end-systolic elastance-effective arterial elastance as an index of ventricular mechanoenergetic performance. *Anesthesiology* 92:1769–1776, 2000. doi:10.1097/00000542-200006000-00037.

[15]Hayashi, Y., M. Takeuchi, H. Takaoka, K. Hata, M. Mori, and M. Yokoyama. Alteration in energetics in patients with left ventricular dysfunction after myocardial infarction: increased oxygen cost of contractility. *Circulation* 93:932–939, 1996.

[16]Hettrick, D. A., P. S. Pagel, D. Lowe, J. P. Tessmer, and D. C. Warltier. Increases in inotropic state without change in heart rate: combined use of dobutamine and zatebradine in conscious dogs. *Eur. J. Pharmacol.* 316:237–244, 1996. doi:10.1016/S0014-2999(96)00688-7.

[17]Hoeksel, S. A., J. A. Blom, J. R. Jansen, J. G. Maessen, and J. J. Schreuder. Automated infusion of vasoactive and inotropic drugs to control arterial and pulmonary pressures during cardiac surgery. *Crit. Care Med.* 27:2792–2798, 1999. doi:10.1097/00003246-199912000-00031.

[18]Iellamo, F., J. A. Sala-Mercado, M. Ichinose, R. L. Hammond, M. Pallante, T. Ichinose, L. W. Stephenson, and D. S. O'Leary. Spontaneous baroreflex control of heart rate during exercise and muscle metaboreflex activation in heart failure. *Am. J. Physiol. Heart Circ. Physiol.* 293:H1929–H1936, 2007. doi:10.1152/ajpheart.00564.2007.

[19]Kim, I. S., H. Izawa, T. Sobue, H. Ishihara, F. Somura, T. Nishizawa, K. Nagata, M. Iwase, and M. Yokota. Prognostic value of mechanical efficiency in ambulatory patients with idiopathic dilated cardiomyopathy in sinus rhythm. *J. Am. Coll. Cardiol.* 39:1264–1268, 2002. doi:10.1016/S0735-1097(02)01775-8.

[20]Knaapen, P., T. Germans, J. Knuuti, W. J. Paulus, P. A. Dijkmans, C. P. Allaart, A. A. Lammertsma, and

F. C. Visser. Myocardial energetics and efficiency: current status of the noninvasive approach. *Circulation* 115:918–927, 2007. doi:10.1161/CIRCULATIONAHA.106.660639.

[21]Miyata, H., E. G. Lakatta, M. D. Stern, and H. S. Silverman. Relation of mitochondrial and cytosolic free calcium to cardiac myocyte recovery after exposure to anoxia. *Circ. Res.* 71:605–613, 1992.

[22]Nikolaidis, L. A., T. Hentosz, A. Doverspike, R. Huerbin, C. Stolarski, Y. T. Shen, and R. P. Shannon. Catecholamine stimulation is associated with impaired myocardial O_2 utilization in heart failure. *Cardiovasc. Res.* 53:392–404, 2002. doi:10.1016/S0008-6363(01)00490-4.

[23]Rao, R. R., B. Aufderheide, and B. W. Bequette. Experimental studies on multiple-model predictive control for automated regulation of hemodynamic variables. *IEEE Trans. Biomed. Eng.* 50:277–288, 2003. doi:10.1109/TBME.2003.808813.

[24]Schipke, J. D., Y. Harasawa, S. Sugiura, J. Alexander, Jr., and D. Burkhoff. Effect of a bradycardic agent on the isolated blood-perfused canine heart. *Cardiovasc. Drugs Ther.* 5:481–488, 1991.

[25]Shen, W., R. M. Gill, B. D. Jones, J. P. Zhang, A. K. Corbly, and M. I. Steinberg. Combined inotropic and bradycardic effects of a sodium channel enhancer in conscious dogs with heart failure: a mechanism for improved myocardial efficiency compared with dobutamine. *J. Pharmacol. Exp. Ther.* 303:673–680, 2002. doi:10.1124/jpet.303.2.673.

[26]Shinke, T., M. Takeuchi, H. Takaoka, and M. Yokoyama. Beneficial effects of heart rate reduction on cardiac mechanics and energetics in patients with left ventricular dysfunction. *Jpn. Circ. J.* 63:957–964, 1999. doi:10.1253/jcj.63.957.

[27]Smiseth, O. A., and O. D. Mjos. A reproducible and stable model of acute ischaemic left ventricular failure in dogs. *Clin. Physiol.* 2:225–239, 1982. doi:10.1111/j.1475-097X.1982.tb00027.x.

[28]Suga, H. Ventricular energetics. *Physiol. Rev.* 70:247–277, 1990.

[29]Suga, H, Y. Yasumura, T. Nozawa, S. Futaki, Y. Igarashi, and Y. Goto. Prospective prediction of O_2 consumption from pressure–volume area in dog hearts. *Am. J. Physiol.* 252:H1258–H1264, 1987.

[30]Uemura, K., A. Kamiya, I. Hidaka, T. Kawada, S. Shimizu, T. Shishido, M. Yoshizawa, M. Sugimachi, and K. Sunagawa. Automated drug delivery system to control systemic arterial pressure, cardiac output, and left heart filling pressure in acute decompensated heart failure. *J. Appl. Physiol.* 100:1278–1286, 2006. doi:10.1152/japplphysiol.01206.2005.

[31]Uemura, K., T. Kawada, A. Kamiya, T. Aiba, I. Hidaka, K. Sunagawa, and M. Sugimachi. Prediction of circulatory equilibrium in response to changes in stressed blood volume. *Am. J. Physiol. Heart Circ. Physiol.* 289:H301–H307, 2005. doi:10.1152/ajpheart.01237.2004.

[32]Uemura, K., M. Sugimachi, T. Kawada, A. Kamiya, Y. Jin, K. Kashihara, and K. Sunagawa. A novel framework of circulatory equilibrium. *Am. J. Physiol. Heart Circ. Physiol.* 286:H2376–H2385, 2004. doi:10.1152/ajpheart.00654.2003.

[33]Yu, C., R. J. Roy, H. Kaufman, and B. W. Bequette. Multiple-model adaptive predictive control of mean arterial pressure and cardiac output. *IEEE Trans. Biomed. Eng.* 39:765–778, 1992. doi:10.1109/10.148385.

Annals of Biomedical Engineering, Vol. 37, No. 1, January 2009 (© 2008) pp. 112–128
DOI: 10.1007/s10439-008-9599-4

Wavelet-Based System Identification of Short-Term Dynamic Characteristics of Arterial Baroreflex

KOJI KASHIHARA,[1,2] TORU KAWADA,[3] MASARU SUGIMACHI,[3] and KENJI SUNAGAWA[4]

[1]Hypertension and Stroke Research Laboratory, Royal North Shore Hospital, University of Sydney, Ground Floor, Building 10, Royal North Shore Hospital, St. Leonards, NSW 2065, Australia; [2]National Institute for Longevity Sciences, NCGG, 36-3 Gengo, Morioka-machi, Obu City, Aichi 474-8511, Japan; [3]Department of Cardiovascular Dynamics, National Cardiovascular Center Research Institute, 5-7-1 Fujishirodai, Suita, Osaka 565-8565, Japan; and [4]Department of Cardiovascular Medicine, Kyushu University, 3-1-1, Maidashi, Higashi-ku, Fukuoka 812-8582, Japan

(Received 1 February 2008; accepted 31 October 2008; published online 12 November 2008)

Abstract—The assessment of arterial baroreflex function in cardiovascular diseases requires quantitative evaluation of dynamic and static baroreflex properties because of the frequent modulation of baroreflex properties with unstable hemodynamics. The purpose of this study was to identify the dynamic baroreflex properties from transient changes of step pressure inputs with background noise during a short-duration baroreflex test in anesthetized rabbits with isolated carotid sinuses, using a modified wavelet-based time-frequency analysis. The proposed analysis was able to identify the transfer function of baroreflex as well as static properties from the transient input-output responses under normal [gain at 0.04 Hz from carotid sinus pressure (CSP) to arterial pressure ($n = 8$); 0.29 ± 0.05 at low (40–60 mmHg), 1.28 ± 0.12 at middle (80–100 mmHg), and 0.38 ± 0.07 at high (120–140 mmHg) CSP changes] and pathophysiological [gain in control vs. phenylbiguanide ($n = 8$); 0.32 ± 0.07 vs. 0.39 ± 0.09 at low, 1.39 ± 0.15 vs. 0.59 ± 0.09 ($p < 0.01$) at middle, and 0.35 ± 0.04 vs. 0.15 ± 0.02 ($p < 0.01$) at high CSP changes] conditions. Subsequently, we tested the proposed wavelet-based method under closed-loop baroreflex responses; the simulation study indicates that it may be applicable to clinical situations for accurate assessment of dynamic baroreflex function. In conclusion, the dynamic baroreflex property to various pressure inputs could be simultaneously extracted from the step responses with background noise.

Keywords—Baroreceptor reflex, Sympathetic nerve activity, Arterial pressure, Transfer function, Dynamic characteristics.

INTRODUCTION

Arterial baroreflex is a crucial negative feedback system because of the quick stabilization of arterial pressure (AP) against external pressure disturbances.[12,30] The assessment of arterial baroreflex function would require quantifying the dynamic as well as static properties[15,46] because the baroreflex gain or sensitivity is frequently modulated during cardiovascular diseases.[6,36,39] Because quick responses of autonomic nerves and AP mainly through the brainstem[3] might contain the unknown characteristics changing by the minute in acute cardiovascular diseases,[25] the short-term dynamic system identification might relate to the novel finding under such nonstationary condition. Laboratory and spontaneous baroreflex methods[37] are widely used in human and animal studies. The laboratory method requires invasive pharmacological or mechanical pressure interventions, and it may be suitable for estimation of the mechanism of AP regulation through the sympathetic as well as vagal baroreflex.[7,45] The spontaneous baroreflex method aims to assess cardiovagal activity noninvasively using systolic AP and heart rate variability.[5] These methods have various merits under the baroreflex testing conditions, but remain debatable because of complicated mechanisms.[27,37,40,43]

In the laboratory method, the standard analysis of sympathetic baroreflex has been performed mainly in the time[10,16] or frequency domain.[1,29,35,44] The time-domain analysis has evaluated the stable or maximal gain around the operating point, but may not characterize the impaired dynamic baroreflex properties accurately in cardiovascular patients with unstable hemodynamics and background noise. In the frequency domain, fast Fourier transform (FFT) analysis[31] has identified dynamic baroreflex properties under such noisy condition, but requires longer data segments to cancel the background noise and to identify the dynamic properties with low-frequency band,[38] indicating difficulties to extract short-term changes. In

Address correspondence to Koji Kashihara, Hypertension and Stroke Research Laboratory, Royal North Shore Hospital, University of Sydney, Ground Floor, Building 10, Royal North Shore Hospital, St. Leonards, NSW 2065, Australia. Electronic mail: kojikasi-nils@umin.ac.jp

0090-6964/09/0100-0112/0 © 2008 Biomedical Engineering Society